# A new a posteriori error estimation for nonlinear time-dependent finite element analysis

Pierre Ladevèze, Nicolas Moës

# A new a posteriori error estimation for nonlinear time-dependent finite element analysis

Pierre Ladevèze*, Nicolas Moës

*Laboratoire de Mécanique et Technologie, E.N.S. Cachan/C.N.R.S./Université Paris 6, 61, Avenue du Président Wilson, Cachan Cedex, France*

In this paper, an error on the constitutive law (labeled the dissipation error) is used to measure the quality of finite element computations of plastic and viscoplastic structures whose behavior is described by internal variables. This measure takes into account all the classical sources of error involved in the computation: the space discretization (the mesh), the time discretization and the iterative technique used to solve the nonlinear discrete problem. More specifically, to quantify the quality of the space and time discretizations, two quantities, called indicators, are introduced. The efficiency of both the error and the indicators is shown for several examples.

## 1. Introduction

Nonlinear finite element analysis for time-dependent problems is quite common nowadays. An important question now is to estimate the quality of these analyses and to minimize the cost of the computation for a given level of accuracy. This paper deals with the first part of the question, i.e. error estimation. Materials described by internal variable formulations (examples: Prandtl–Reuss model for plasticity, Chaboche model for viscoplasticity [1], etc.) are considered. There is growing interest for this kind of formulation at the theoretical, experimental and computational levels. The assumptions of small strains and displacements, as well as isothermal and quasi-static loading, are made.

Many papers have dealt with error estimation for linear problems. Three main differing approaches must be distinguished. The first one, chronologically speaking, is based on the concept of error on the constitutive law [2] and has been applied, among other areas, to thermal [2] and elastic problems [3]. The second one, introduced by Babuska and Rheinboldt [4,5], then developed by Zienkiewicz et al. [6,7] and more recently by Oden et al. [8], uses the equilibrium residuals through local problems to estimate the error. The last one, developed by Zienkiewicz and Zhu [9–11], consists in comparing the finite element solution to a smoother one obtained by special averaging techniques. Finally, let us mention the dual analysis approach based on upper and lower bounds for the energy [12,13]. A validation of these a posteriori error estimators can be found in [14–16].

In comparison with the linear case, much less has been accomplished for the nonlinear case. For nonlinear time-independent problems, Babuska [17] and Johnson [18] have designed error estimates for nonlinear elasticity and Hencky-type plasticity, respectively. For nonlinear time-dependent problems, techniques devised for linear problems or time-independent nonlinear problems are used at each time step [19–21]. Unfortunately, the error estimates so built do not take into account the errors due to the time discretization. In a time-dependent

* Corresponding author.

nonlinear problem, the quality of the finite element solution at time $t$ depends indeed, not only upon the quality of the mesh, but also on the two following influences: the quality of the time discretization performed since the beginning of the loading, and the defect of convergence of the global iterative algorithm at each computed time (Newton's algorithm, for instance).

An error on the constitutive law taking into account the three sources of error described previously has been proposed by Ladevèze [22]. This measure, based on Drucker's inequality, was first applied in [23] for plane stress problems and three-node triangles. In this paper, a procedure to adapt the mesh is also described. The Drucker error has recently been reused and enhanced in order to conduct a simultaneous adaptive control of the space and time discretization for three and six-node triangles in plane and axisymmetric problems [24]. The Drucker error is based on a sufficient condition that ensures the stability of the material.

In this paper, we introduce and implement new a posteriori error estimates to characterize the quality of finite element calculations that are based upon the notion of dissipation errors as elaborated in [25] and [26]. This approach is designed for more common situations where the state of the material is described by a set of internal variables (plastic strain, hardening parameters, . . .). With this modeling approach being much more mechanical in nature, it is taking a step over the functional description of the material. The key idea herein is to divide the equations of the problem into two groups:

- A group of equations related to the free energy including the equation of equilibrium, the kinetic constraints, the state laws and the initial conditions.
- A group of equations related to the dissipation, i.e. the constitutive laws describing the evolution of the material state.

The dissipation error characterizes the quality of an approximate admissible solution, i.e. a solution satisfying the first group of equations. This quality is quantified by the non-verification of the second group of equations. This fact naturally leads to the terminology of dissipation error. The finite element solution is of course not admissible. Thus, an important task is to elaborate, at low cost, a strictly admissible solution. Another important task is to define the error's measure. We will be mainly concerned here with the class of standard materials covering most of the plastic and viscoplastic materials. The extension of the notion of dissipation error to non-standard materials do not lead a priori to further difficulties, for instance by using the concept of bipotential [27,28]. An advantage of the dissipation error is that it is directly linked to a gap between the exact and the approximated solutions. This result, analogous to the Prager–Synge theorem for elasticity, is demonstrated in [26].

Let us now focus on the contents of this paper. The reference problem and the dissipation errors are described in Sections 2 and 3, respectively. The usefulness of such a posteriori error estimations is evaluated in the framework of the classical incremental finite element method in Section 4 and illustrated for several examples in Section 5. As for the Drucker error, the dissipation error does take into account all the error sources involved in the computation. It is useful, for an adaptive control, for instance, to distinguish within the error the part due to the mesh from the one due to the time discretization. Two indicators are introduced for this purpose and tested in Section 6.

## 2. The continuous reference problem

Concerning the notations, vectors will be underlined ($\underline{U}, \underline{U}^*, \ldots$) and second-order tensors bold italic. For instance, strains and stresses will be denoted by $\boldsymbol{\sigma}$ and $\boldsymbol{\varepsilon}$, respectively. This notation will also be used to denote the additional internal variables. For more complex operators, such as Hooke's tensor, they will be in bold roman, such as $\mathbf{K}$. And finally, the first derivative of a function $f$ with scalar argument will be denoted by $f'$.

The solid medium under study occupies at the initial time so as for the further moments (small strain and displacement assumption) a domain $\Omega$ bounded by $\partial\Omega$. The study is carried out over the time interval $[0, T]$. The environment of the medium is schematised for all $t$ belonging to $[0, T]$ with an imposed displacement $\underline{U}_d$ on a part $\partial_1\Omega$ of the boundary, a surfacic load $\underline{F}_d$ on $\partial_2\Omega$ (complementary to $\partial_1\Omega$) and a volumic load $\underline{f}_d$ on the domain $\Omega$. We will assume, without any loss of generality, that the partition of $\partial\Omega$ in $\partial_1\Omega$ and $\partial_2\Omega$ is constant with respect to time. The desired solution must fulfill the kinematic constraints, the equilibrium equation, the constitutive law and the initial conditions. Concerning the regularity imposed on the displacements, speeds, stress, . . . i.e. the spaces where these fields are to be found, we will work in the usual bounded energy frame.

For more details, see for instance [29]. $\mathcal{U}$ will denote the space where we look for the displacement field $\underline{U}$ defined on $\Omega$ and $\mathcal{S}$ the space where we look for the stress field, also defined on $\Omega$. The extension of these two spaces to the whole time $[0, T]$ will be denoted $\mathcal{U}^{[0,T]}$ and $\mathcal{S}^{[0,T]}$, respectively. Finally, Tr stands for the trace.

*2.1. The kinematic constraints*

$$\underline{U} \in \mathcal{U}_{\text{ad}}^{[0,T]} \tag{1}$$

$$\mathcal{U}_{\text{ad}}^{[0,T]} = \{\underline{U} \in \mathcal{U}^{[0,T]} \text{ such that } \underline{U} = \underline{U}_d \text{ on } [0, T] \times \partial_1 \Omega\} \tag{2}$$

Let us also define the set $\mathcal{U}_0$:

$$\mathcal{U}_0 = \{\underline{\underline{U}} \in \mathcal{U} \text{ such that } \underline{U} = 0 \quad \text{on } \partial_1 \Omega\} \tag{3}$$

*2.2. The equilibrium equations (in quasi-static)*

$$\boldsymbol{\sigma} \in \mathcal{S}_{\text{ad}}^{[0,T]} \tag{4}$$

$$\mathcal{S}_{\text{ad}}^{[0,T]} = \{\boldsymbol{\sigma} \in \mathcal{S}^{[0,T]} \text{ satisfying (5) } \forall\, \underline{U}^* \in \mathcal{U}_0 \text{ and } \forall\, t \in [0, T]\}$$

$$\int_\Omega \text{Tr}[\boldsymbol{\sigma}\boldsymbol{\varepsilon}(\underline{U}^*)]\, \mathrm{d}\Omega - \int_\Omega \underline{f}_d \circ \underline{U}^*\, \mathrm{d}\Omega - \int_{\partial_2 \Omega} \underline{F}_d \circ \underline{U}^*\, \mathrm{d}S = 0 \tag{5}$$

*2.3. The behavior described by internal variables*

The state of the material is characterized at each point by the total strain $\boldsymbol{\varepsilon}$, the inelastic strain $\boldsymbol{\varepsilon}^p$ and a set of internal variables denoted by $\boldsymbol{X}$. The associated variables are the stress for $\boldsymbol{\varepsilon}$ and $\boldsymbol{\varepsilon}^p$, and the quantity $\boldsymbol{Y}$ for $\boldsymbol{X}$. Thus, the expression of the dissipation is

$$\text{Tr}[\boldsymbol{\sigma}\dot{\boldsymbol{\varepsilon}}^p] - \boldsymbol{Y} \circ \dot{\boldsymbol{X}} \tag{6}$$

The second term specifies the contribution of $(\boldsymbol{X}, \boldsymbol{Y})$ to the dissipation. If $\boldsymbol{X}$ denotes a column of $\boldsymbol{R}^n$, then $\boldsymbol{Y}$ is also a column of $\boldsymbol{R}^n$ and we have

$$\boldsymbol{Y} \circ \dot{\boldsymbol{X}} = \boldsymbol{Y}^t \dot{\boldsymbol{X}}$$

where t stands for the usual transposition. More precisely, two space $\mathbf{e}$ and $\mathbf{f}$ are placed in duality by the following bilinear form:

$$\begin{bmatrix} \dot{\boldsymbol{\varepsilon}}^p \\ -\dot{\boldsymbol{X}} \end{bmatrix}, \begin{bmatrix} \boldsymbol{\sigma} \\ \boldsymbol{Y} \end{bmatrix} \rightarrow \text{Tr}[\boldsymbol{\sigma}\dot{\boldsymbol{\varepsilon}}^p] - \boldsymbol{Y} \circ \dot{\boldsymbol{X}}$$

$$\mathbf{e} \times \mathbf{f} \quad \rightarrow \quad \boldsymbol{R}$$

As we work with the small strain assumption, the total strain is the symmetric part of the gradient of $\underline{U}$. In an orthonormed basis, one has

$$[\boldsymbol{\varepsilon}(\underline{U})]_{ij} = \frac{1}{2}(U_{i,j} + U_{j,i})$$

and we have the additivity relation of the rate of elastic $\dot{\boldsymbol{\varepsilon}}^e$ and inelastic $\dot{\boldsymbol{\varepsilon}}^p$ strains: $\dot{\boldsymbol{\varepsilon}} = \dot{\boldsymbol{\varepsilon}}^e + \dot{\boldsymbol{\varepsilon}}^p$.

*2.3.1. The state laws*

According to the first principle of thermodynamics, a free energy $\psi$, depending only on the state variables $\boldsymbol{\varepsilon}$, $\boldsymbol{\varepsilon}^p$ and $\boldsymbol{X}$, can be introduced. The following classical assumptions are made:

- $\psi$ depends only upon the elastic strain $\boldsymbol{\varepsilon}^e$ and the internal variables $\boldsymbol{X}$.
- $\psi(\boldsymbol{\varepsilon}^e, \boldsymbol{X}) = \psi_e(\boldsymbol{\varepsilon}^e) + \psi_p(\boldsymbol{X})$
- Elasticity is linear: $\psi_e(\boldsymbol{\varepsilon}^e) = \frac{1}{2}\text{Tr}[\mathbf{K}\boldsymbol{\varepsilon}^e\boldsymbol{\varepsilon}^e]$, where $\mathbf{K}$ is Hooke's tensor.

The derivation of $\psi$ yields the state laws $\boldsymbol{\sigma} = \mathbf{K}\boldsymbol{\varepsilon}^e$ and $\boldsymbol{Y} = \mathbf{G}(\boldsymbol{X})$, where $\mathbf{G}(\boldsymbol{X})$ is the derivative of $\psi_p$ with respect to $\boldsymbol{X}$.

*2.3.2. The evolution laws*

The fulfillment of the second principle of thermodynamics, written as follows:

$$\mathrm{Tr}[\dot{\boldsymbol{\sigma}}\boldsymbol{\varepsilon}^p] - \boldsymbol{Y} \circ \dot{\boldsymbol{X}} \geqslant 0$$

warrants including in the model a relation between $(\dot{\boldsymbol{\varepsilon}}^p, -\dot{\boldsymbol{X}})$ and $(\boldsymbol{\sigma}, \boldsymbol{Y})$, in other words an evolution law for the internal variables $(\boldsymbol{\varepsilon}^p, \boldsymbol{X})$. Formally, one can write

$$\begin{bmatrix} \dot{\boldsymbol{\varepsilon}}^p \\ -\dot{\boldsymbol{X}} \end{bmatrix} = B\left(\begin{bmatrix} \boldsymbol{\sigma} \\ \boldsymbol{Y} \end{bmatrix}\right) \qquad \boldsymbol{\varepsilon}^p = 0\,, \quad \boldsymbol{X} = 0 \quad \text{for } t = 0 \tag{7}$$

$B$ is an operator relevant to the material. It must be positive to respect the second principle of thermodynamics. The material is suppose to be initially virgin. $E$ will denote the space where the fields $(\dot{\boldsymbol{\varepsilon}}^p, -\dot{\boldsymbol{X}})$ defined on $\Omega$ are to be found and $E^{[0,T]}$ the history of these fields on $[0, T]$. The corresponding space for the dual fields are denoted by $F$ and $F^{[0,T]}$, respectively.

*2.3.3. Standard materials*

A typical way to define the operator $B$ is to give a scalar function $\varphi^*(\boldsymbol{\sigma}, \boldsymbol{Y})$, generally convex, called the potential of dissipation, and to write

$$\begin{pmatrix} \dot{\boldsymbol{\varepsilon}}^p \\ -\dot{\boldsymbol{X}} \end{pmatrix} \in \begin{pmatrix} \partial_{\boldsymbol{\sigma}} \varphi^*(\boldsymbol{\sigma}, \boldsymbol{Y}) \\ \partial_{\boldsymbol{Y}} \varphi^*(\boldsymbol{\sigma}, \boldsymbol{Y}) \end{pmatrix} \tag{8}$$

where $(\partial_{\boldsymbol{\sigma}}\varphi^*, \partial_{\boldsymbol{Y}}\varphi^*)$ denotes the subdifferential of $\varphi^*$ at $(\boldsymbol{\sigma}, \boldsymbol{Y})$. When the potential is differentiable, the subdifferential becomes a classical gradient and the membership sign an equality. A model for which the evolution laws are given by the subdifferential of a dissipation potential (8) is called standard for the choice of variables $(\boldsymbol{X}, \boldsymbol{Y})$. The interest of a standard model lies in the following classical property. The second principle of thermodynamics is fulfilled if one has a potential satisfying:

$$\varphi^* \text{ convex} \qquad \varphi^*(0, 0) = 0 \qquad \varphi^*(\bullet, \bullet) \geqslant 0 \tag{9}$$

*2.3.4. Examples of standard materials*

As an example, let us consider the Prandtl–Reuss plastic model and its viscoplastic version. Besides the plastic strain, the model involves another scalar internal variable $p$ that can be interpreted as the cumulative plastic strain. The free energy is of the form:

$$\psi(\boldsymbol{\varepsilon}^e, p) = \frac{1}{2}\mathrm{Tr}[\mathbf{K}\boldsymbol{\varepsilon}^e\boldsymbol{\varepsilon}^e] + g(p)$$

where $g$ is a function characterizing the hardening law. So,

$$\boldsymbol{\sigma} = \mathbf{K}\boldsymbol{\varepsilon}^e \qquad R = g'(p) \tag{10}$$

These are different classical hardening laws: $R = k_y p$ (linear hardening), $R = k_y p^{1/m}$ (power hardening) and $R = R_M(1 - \exp(-\gamma p))$ (exponential hardening). $k_y, m, R_M, \gamma$ are constant material parameters. As for all standard plastic models, the dissipation potential is the indicator function of the convex of elasticity. Such a function is zero in the convex of elasticity and $+\infty$ elsewhere. Here, the convex of elasticity is the set $(\boldsymbol{\sigma}, \boldsymbol{Y})$ satisfying:

$$z(\boldsymbol{\sigma}, R) = \|\boldsymbol{\sigma}^D\| - (R + R_0) \leqslant 0$$

where $\boldsymbol{\sigma}^D$ is the deviator of the stresses, $\|\boldsymbol{\sigma}^D\|$ its norm and $R_0$ the initial yield stress.

$$\|\boldsymbol{\sigma}^D\| = (\mathrm{Tr}[\boldsymbol{\sigma}^D\boldsymbol{\sigma}^D])^{1/2}$$

One may easily check that $\varphi^*$ fulfills the sufficient conditions (9) ensuring the respect of the second thermodynamics principle. A viscoplastic version of the Prandtl–Reuss plastic model is obtained by the regularization of the plastic potential; for instance, with a power law:

$$\varphi^*(\boldsymbol{\sigma}, R) = \frac{k}{n+1}\langle z \rangle_+^{n+1} \tag{11}$$

where $\langle z \rangle_+$ denotes the positive part of $z$: $\langle z \rangle_+ = (z + |z|)/2$.

*2.3.5. Non-standard materials described with a bipotential*

Some typical material behaviors cannot be described in a standard way. For some of these materials, such as the Coulomb's dry friction and the nonlinear kinematical hardening rule for cyclic plasticity of metals presented by Chaboche [1], evolution laws may be written in an elegant way using the bipotential notion introduced by de Saxcé [27] that generalizes, in some way, the notion of potential to the non-standard materials case. A bipotential is a scalar function $b([\dot{\boldsymbol{\varepsilon}}^p, -\dot{\boldsymbol{X}}], [\boldsymbol{\sigma}, \boldsymbol{Y}])$ satisfying the following conditions:

- $b$ is convex with respect to both its arguments taken separately, i.e. $b(\bullet, [\boldsymbol{\sigma}, \boldsymbol{Y}])$ and $b([\dot{\boldsymbol{\varepsilon}}^p, -\dot{\boldsymbol{X}}], \bullet)$ are convex for all $(\dot{\boldsymbol{\varepsilon}}^p, -\dot{\boldsymbol{X}}, \boldsymbol{\sigma}, \boldsymbol{Y})$.
- $b([\dot{\boldsymbol{\varepsilon}}^p, -\dot{\boldsymbol{X}}], [\boldsymbol{\sigma}, \boldsymbol{Y}]) - \mathrm{Tr}[\boldsymbol{\sigma}\dot{\boldsymbol{\varepsilon}}^p] + \boldsymbol{Y} \circ \dot{\boldsymbol{X}} \geqslant 0 \quad \forall (\dot{\boldsymbol{\varepsilon}}^p, -\dot{\boldsymbol{X}}, \boldsymbol{\sigma}, \boldsymbol{Y})$
- Evolution laws are given by
  $b([\dot{\boldsymbol{\varepsilon}}^p, -\dot{\boldsymbol{X}}], [\boldsymbol{\sigma}, \boldsymbol{Y}]) - \mathrm{Tr}[\boldsymbol{\sigma}\dot{\boldsymbol{\varepsilon}}^p] + \boldsymbol{Y} \circ \dot{\boldsymbol{X}} = 0.$

*2.3.6. Formulation of the behavior*

In summary, the state of the material is defined by the total strain $\boldsymbol{\varepsilon}$, the inelastic strain $\boldsymbol{\varepsilon}^p$ and the internal variables $\boldsymbol{X}$. The dual quantities are $\boldsymbol{\sigma}$ and $\boldsymbol{Y}$. The constitutive laws are

*The state laws*:

$$\boldsymbol{\sigma} = \mathbf{K}(\boldsymbol{\varepsilon} - \boldsymbol{\varepsilon}^p) \qquad \boldsymbol{Y} = \mathbf{G}(\boldsymbol{X}) \tag{12}$$

*The evolution laws and initial conditions*:

$$\begin{bmatrix} \dot{\boldsymbol{\varepsilon}}^p \\ -\dot{\boldsymbol{X}} \end{bmatrix} \in B\left(\begin{bmatrix} \boldsymbol{\sigma} \\ \boldsymbol{Y} \end{bmatrix}\right) \qquad \boldsymbol{\varepsilon}^p = 0, \boldsymbol{X} = 0 \quad \text{for } t = 0 \tag{13}$$

If the model is standard, $B$ is derived from a potential $\varphi^*(\boldsymbol{\sigma}, \boldsymbol{Y})$, i.e.

$$\begin{bmatrix} \dot{\boldsymbol{\varepsilon}}^p \\ -\dot{\boldsymbol{X}} \end{bmatrix} \in \begin{bmatrix} \partial_{\boldsymbol{\sigma}} \varphi^*(\boldsymbol{\sigma}, \boldsymbol{Y}) \\ \partial_{\boldsymbol{Y}} \varphi^*(\boldsymbol{\sigma}, \boldsymbol{Y}) \end{bmatrix} \qquad \boldsymbol{\varepsilon}^p = 0, \boldsymbol{X} = 0 \quad \text{for } t = 0 \tag{14}$$

Eliminating the variables $\boldsymbol{X}$, $\boldsymbol{Y}$ and $\boldsymbol{\varepsilon}^p$, one gets the functional formulation of the constitutive law:

$$\boldsymbol{\sigma}(t) = \mathscr{A}(\dot{\boldsymbol{\varepsilon}}(\tau), \tau \leqslant t) \quad t \in [0, T] \tag{15}$$

*2.4. Normal formulation of a constitutive law*

Herein, we sum up the discussion about the choice of the internal variables given in [25]. Consider two sets of internal variables $(\boldsymbol{X}, \boldsymbol{Y})$ and $(\underset{\sim}{\boldsymbol{X}}, \underset{\sim}{\boldsymbol{Y}})$ linked by the following change of variables:

$$\underset{\sim}{\boldsymbol{X}} = R(\boldsymbol{X}) \qquad \underset{\sim}{\boldsymbol{Y}} = S(\boldsymbol{Y}) \tag{16}$$

and suppose this change does not modify the functional law (15). Why should one choose to formulate the behavior with the set $(\boldsymbol{X}, \boldsymbol{Y})$ instead of the set $(\underset{\sim}{\boldsymbol{X}}, \underset{\sim}{\boldsymbol{Y}})$? The significance of the variables or the dissipation's value may help to decide. Although leading to the same functional law, the dissipation value is indeed in general modified by the variable change, i.e. $-\boldsymbol{Y} \circ \dot{\boldsymbol{X}} \neq -\underset{\sim}{\boldsymbol{Y}} \circ \dot{\underset{\sim}{\boldsymbol{X}}}$. If we fail to take into account these two arguments, there is no reason to favor one set of variables over the other. A formulation in which the variables $\boldsymbol{X}$ and $\boldsymbol{Y}$ have the same weight, i.e. linked by a linear relationship, is said to be normal. Such a formulation is given by

$$\boldsymbol{\sigma} = \mathbf{K}(\boldsymbol{\varepsilon} - \boldsymbol{\varepsilon}^p) \qquad \underset{\sim}{\boldsymbol{Y}} = \boldsymbol{\Lambda} \underset{\sim}{\boldsymbol{X}} \tag{17}$$

$$\begin{bmatrix} \dot{\boldsymbol{\varepsilon}}^p \\ -\dot{\underset{\sim}{\boldsymbol{X}}} \end{bmatrix} = B\left(\begin{bmatrix} \boldsymbol{\sigma} \\ \underset{\sim}{\boldsymbol{Y}} \end{bmatrix}\right) \qquad \underset{\sim}{\boldsymbol{X}} = 0, \boldsymbol{\varepsilon}^p = 0, \quad \text{for } t = 0 \tag{18}$$

where $\boldsymbol{\Lambda}$ is a constant symmetric linear definite positive operator. In [25], the following results have been proven:

- Every model of the type (12)–(13) implies a normal formulation.

- A standard material admits a normal *standard* formulation if some conditions that are not too restrictive in practice, hold. These conditions are necessary to preserve the standard initial standard character of the formulation when writing to the normal one.
- Every bistandard material implies a standard normal formulation. A material model is said to be bistandard if it is standard and fulfills the following conditions for the variable sets $(\boldsymbol{Y}, \dot{\boldsymbol{X}})$ and $(\boldsymbol{X}, \dot{\boldsymbol{Y}})$:
  - $\varphi^*(\boldsymbol{\sigma}, \boldsymbol{Y})$, $\varphi^*(\boldsymbol{\sigma}, \mathbf{G}(\boldsymbol{X}))$: convex functions
  - $\varphi^*(0, 0) = 0$, $\varphi^* \geqslant 0$, $\mathbf{G}(0) = 0$
  - $\psi(\boldsymbol{\varepsilon}^e, \boldsymbol{X}) = \psi_e(\boldsymbol{\varepsilon}^e) + \psi_p(\boldsymbol{X})$: convex function

  *Remark*: a normal standard formulation is trivially bistandard.

*2.4.1. Examples of normal standard formulation*

If $k_y > 0$, $m > 1$, $R_M > 0$, $\gamma > 0$, $k > 0$, $n > 0$, all the models earlier described are bistandard and thus implies a normal standard formulation. This formulation reads

$$\boldsymbol{\sigma} = \mathbf{K}(\boldsymbol{\varepsilon} - \boldsymbol{\varepsilon}^p) \qquad \underset{\sim}{R} = \lambda \underset{\sim}{p} \tag{19}$$

Now,

$$z(\boldsymbol{\sigma}, \underset{\sim}{R}) = \|\boldsymbol{\sigma}^D\| - (l(\underset{\sim}{R}) + R_0) \leqslant 0$$

For the power hardening law:

$$l(\underset{\sim}{R}) = \frac{1}{\alpha + 1} \underset{\sim}{R}^{\alpha + 1} \quad \text{with} \quad \lambda = \frac{1}{1 - \alpha} ((\alpha + 1) k_y)^{(1-\alpha)/(1+\alpha)} \quad \text{and} \quad \alpha = \frac{1 - m}{1 + m}$$

And for the exponential hardening law:

$$l(\underset{\sim}{R}) = \underset{\sim}{R}\left(1 - \frac{1}{4R_M} \underset{\sim}{R}\right) \quad \text{with} \quad \lambda = R_M \gamma$$

In plasticity, the dissipation potential is the indicator function of the convex domain defined by $z \leqslant 0$ and in viscoplasticity, the expression (11) must be used. For a linear hardening law, the initial formulation is of course already normal (and standard).

The next section is devoted to the dissipation error. First, the basic concepts are presented in detail. Then, we will see how these concepts may be applied to normal standard, bistandard and non-standard formulations.

## 3. The dissipation error: concepts and measurements

The notion of error on the constitutive law has been introduced in [30]. It relies on splitting the equations of the problem into two groups. When the behavior is formulated by a functional law, the first group combines both the equilibrium equations and the kinematic constraints, and the second group contains the constitutive law. The quality of an approximate solution satisfying the first group (i.e. and admissible solution) is quantified by the non-fulfillment of the second group of equations (constitutive law). If Drucker's stability inequality holds for the material, a natural way to measure the error can be obtained [23,24]. The error on the constitutive relation is a very mechanical approach since less confidence is given to the behavior of the material.

When the state of the material is described by internal variables, the admissibility notion must be revised. Indeed, the state laws, associated with the free energy, and the evolution laws, associated with the dissipative phenomena, must be distinguished in the formulation. In [26], the choice has been made to include the state laws in the definition of admissibility, with the error being measured on the evolution laws alone. The problem is divided precisely into two groups:

- The first group defines the admissibility of a solution. It combines the equations related to the free energy: the equilibrium equation, the kinematic constraints and the state laws $\boldsymbol{\sigma} = \mathbf{K}(\boldsymbol{\varepsilon} - \boldsymbol{\varepsilon}^p)$ and $\boldsymbol{Y} = \mathbf{G}(\boldsymbol{X})$. We also add to this group the initial conditions (defining the initial state of the material, taken here as virgin) $(\boldsymbol{\varepsilon}^p, \boldsymbol{X}) = 0$ at $t = 0$ on $\Omega$.
- The second group, related to the dissipation, only includes the evolution laws.

Two questions must be still answered to actually utilize the dissipation error concept. The first one deals with

the admissibility. In general, the finite element solution obtained from the computation is not admissible. For instance, the stresses are not exactly statically admissible. The construction of an admissible solution from the finite element one will be addressed in Section 4. The second question, that concerns the definition itself of the error measurement, is the topic of the next section. The measurement depends upon the type of formulation considered. If the material is standard, or more generally bistandard, a measurement is given by the inequality property of the Legendre-Fenchel transform. If the material is not standard but admits a bipotential, properties of the bipotential may be used. In the more general case, the measurement should use the monotony property of the operator $B$.

### *3.1. Classical properties of standard formulations*

With the help of the Legendre–Fenchel transform, one can associate a dual potential $\varphi(\dot{\boldsymbol{\varepsilon}}^p, -\dot{\boldsymbol{X}})$ to the primal one $\varphi^*(\boldsymbol{\sigma}, \boldsymbol{Y})$.

$$\varphi(\dot{\boldsymbol{\varepsilon}}^p, -\dot{\boldsymbol{X}}) \equiv \sup_{(\boldsymbol{\sigma},\boldsymbol{Y})\in\mathbf{f}} (\mathrm{Tr}[\boldsymbol{\sigma}\dot{\boldsymbol{\varepsilon}}^p] - \boldsymbol{Y}\circ\dot{\boldsymbol{X}} - \varphi^*(\boldsymbol{\sigma}, \boldsymbol{Y})) \tag{20}$$

The Legendre–Fenchel transform possesses two interesting classical properties:

$$\eta(\dot{\boldsymbol{\varepsilon}}^p, \dot{\boldsymbol{X}}, \boldsymbol{\sigma}, \boldsymbol{Y}) \geqslant 0 \quad \forall\, (\boldsymbol{\sigma}, \boldsymbol{Y}, \dot{\boldsymbol{\varepsilon}}^p, -\dot{\boldsymbol{X}}) \tag{21}$$

$$\eta(\dot{\boldsymbol{\varepsilon}}^p, \dot{\boldsymbol{X}}, \boldsymbol{\sigma}, \boldsymbol{Y}) = 0 \quad \Leftrightarrow \quad \begin{pmatrix} \dot{\boldsymbol{\varepsilon}}^p \\ -\dot{\boldsymbol{X}} \end{pmatrix} \in \begin{pmatrix} \partial_{\boldsymbol{\sigma}}\varphi^*(\boldsymbol{\sigma}, \boldsymbol{Y}) \\ \partial_{\boldsymbol{Y}}\varphi^*(\boldsymbol{\sigma}, \boldsymbol{Y}) \end{pmatrix} \tag{22}$$

The condensed following notation has been used:

$$\eta(\dot{\boldsymbol{\varepsilon}}^p, \dot{\boldsymbol{X}}, \boldsymbol{\sigma}, \boldsymbol{Y}) \equiv \varphi(\dot{\boldsymbol{\varepsilon}}^p, -\dot{\boldsymbol{X}}) + \varphi^*(\boldsymbol{\sigma}, \boldsymbol{Y}) - \mathrm{Tr}[\boldsymbol{\sigma}\dot{\boldsymbol{\varepsilon}}^p] + \boldsymbol{Y}\circ\dot{\boldsymbol{X}} \tag{23}$$

The inequality (21) is usually called the Legendre–Fenchel inequality, and the equality relation (22) simply means that $\eta$ is zero if and only if the evolution laws are satisfied.

### *3.2. Error measurement for standard model with normal formulation*

The quantity $\eta$ allows measuring at each time and each place the quality of compliance with the evolution laws. The absolute error $e$ can thus be defined as follows:

$$e \equiv \int_0^T \int_\Omega \eta(\dot{\boldsymbol{\varepsilon}}^p, \dot{\boldsymbol{X}}, \boldsymbol{\sigma}, \boldsymbol{Y})\, \mathrm{d}\Omega\, \mathrm{d}t \tag{24}$$

The absolute error is zero if and only if the admissible solution and the exact solution both coincide on $[0, T]$. The norm chosen allows writing a direct link between the error and the gap occuring between the exact and admissible solutions.

*PROPERTY 1*

$$e = \int_0^T \int_\Omega \eta(\overline{\dot{\boldsymbol{\varepsilon}}^p}, \overline{\dot{\boldsymbol{X}}}, \boldsymbol{\sigma}, \boldsymbol{Y}) + \eta(\dot{\boldsymbol{\varepsilon}}^p, \dot{\boldsymbol{X}}, \overline{\boldsymbol{\sigma}}, \overline{\boldsymbol{Y}})\, \mathrm{d}\Omega\, \mathrm{d}t$$
$$+ \frac{1}{2}\int_\Omega \mathrm{Tr}[\mathbf{K}^{-1}(\boldsymbol{\sigma} - \overline{\boldsymbol{\sigma}})(\boldsymbol{\sigma} - \overline{\boldsymbol{\sigma}})] + \boldsymbol{\Lambda}^{-1}(\boldsymbol{Y} - \overline{\boldsymbol{Y}})\circ(\boldsymbol{Y} - \overline{\boldsymbol{Y}})\, \mathrm{d}\Omega\big|_T$$

$(\overline{\dot{\boldsymbol{\varepsilon}}^p}, \overline{\dot{\boldsymbol{X}}}, \overline{\boldsymbol{\sigma}}, \overline{\boldsymbol{Y}})$ denotes the exact solution and $(\dot{\boldsymbol{\varepsilon}}^p, \dot{\boldsymbol{X}}, \boldsymbol{\sigma}, \boldsymbol{Y})$ the admissible one. This property has been established in [26] and is an extension of the famous Prager–Synge theorem [31].

#### *3.2.1. Absolute and relative error*

The relative error $\epsilon$ is defined by $\epsilon = e/D$ where

$$D \equiv 4 \sup_{t\in[0,T]} d_t \tag{25}$$

$$d_t \equiv (1-\gamma)\int_0^t\int_\Omega [\varphi^*(\boldsymbol{\sigma}, \boldsymbol{Y}) + \varphi(\dot{\boldsymbol{\varepsilon}}^p, \dot{\boldsymbol{X}})]\,\mathrm{d}\Omega\,\mathrm{d}t + \gamma\int_\Omega \frac{1}{2}\mathrm{Tr}[\mathbf{K}^{-1}\boldsymbol{\sigma}\boldsymbol{\sigma}] + \frac{1}{2}\boldsymbol{\Lambda}^{-1}\boldsymbol{Y}\circ\boldsymbol{Y}\,\mathrm{d}\Omega\Big|_t \tag{26}$$

The $\gamma$ parameter ($0 \leqslant \gamma \leqslant 1$) allows weighting the values of the dissipation and the free energy in the denominator. We set $\gamma = \frac{1}{2}$. For pure elastic problems, the dissipation tends to zero and the denominator becomes dramatically small compared to the numerator. Thus, we impose a minimum value for the dissipation given by

$$\frac{R_0}{\|\boldsymbol{\sigma}^D\|}\,|\dot{\psi}_e(\boldsymbol{\varepsilon}^e)|$$

where $|\dot{\psi}_e|$ is the absolute value of the derivative with respect to time of the elastic free energy. This choice leads to reasonable dissipation error in elasticity in comparison to classical error norm for such problems. So, $d_t$ is now defined by

$$d_t \equiv (1-\gamma)\int_0^t\int_\Omega \sup\left[(\varphi^*(\boldsymbol{\sigma}, \boldsymbol{Y}) + \varphi(\dot{\boldsymbol{\varepsilon}}^p, \dot{\boldsymbol{X}})), \frac{R_0}{\|\boldsymbol{\sigma}^D\|}\,|\dot{\psi}_e(\boldsymbol{\varepsilon}^e)|\right]\mathrm{d}\Omega\,\mathrm{d}t$$
$$+\gamma\int_\Omega \frac{1}{2}\mathrm{Tr}[\mathbf{K}^{-1}\boldsymbol{\sigma}\boldsymbol{\sigma}] + \frac{1}{2}\boldsymbol{\Lambda}^{-1}\boldsymbol{Y}\circ\boldsymbol{Y}\,\mathrm{d}\Omega\Big|_t$$

*3.2.2. Global error and local contributions*

Due to the simple norm chosen, it is easy to express the global error $\boldsymbol{\epsilon}$ in terms of local contributions. The local contribution to the error of the space–time domain $\omega_i$ ($\omega_i \subset [0,T]\times\Omega$) is defined by

$$\boldsymbol{\epsilon}_{\omega_i} \equiv \frac{\int_{\omega_i}\eta\,\mathrm{d}\omega_i}{D} \tag{27}$$

If the set of $\omega_i$, $i = 1, \ldots, I$ is a partition of $[0,T]\times\Omega$ (i.e. $\cup_{i=1}^{I}\omega_i = [0,T]\times\Omega$ and $\omega_i \cap \omega_j = \emptyset$ for $i \neq j$), we have

$$\boldsymbol{\epsilon} = \sum_{i=1}^{I}\boldsymbol{\epsilon}_{\omega_i} \tag{28}$$

In the finite element computation case, the time–space domain is naturally divided into elements $E$ and time steps $\Delta t$. Whether $\omega$ denotes $\Delta t\times E$, $\Delta t\times\Omega$ or $[0,T]\times E$, $\boldsymbol{\epsilon}_\omega$ will represent the contribution to the error of a time step over an element, a time step over the whole structure or an element over the whole time period, respectively. Finally, if $\varphi$ denotes $[0,t]\times\Omega$, we obtain the contribution of the time interval $[0,t]$ over the whole structure:

$$\boldsymbol{\epsilon}_{[0,t]\times\Omega} \equiv \frac{\int_0^t\int_\Omega \eta\,\mathrm{d}\Omega\,\mathrm{d}t}{D} \tag{29}$$

*3.3. Error measurement for bistandard model*

For bistandard formulations, a link between the error and the gap occuring between the exact and admissible solutions still exists [26]. $(\overline{\dot{\boldsymbol{\varepsilon}}^p}, \dot{\overline{\boldsymbol{X}}}, \overline{\boldsymbol{\sigma}}, \overline{\boldsymbol{Y}})$ again denotes the exact solution and $(\dot{\boldsymbol{\varepsilon}}^p, \dot{\boldsymbol{X}}, \boldsymbol{\sigma}, \boldsymbol{Y})$ the admissible one.

*PROPERTY 2*

$$\underset{\sim}{e} = \frac{1}{2}\int_0^T\int_\Omega \eta(\overline{\dot{\boldsymbol{\varepsilon}}^p}, \dot{\overline{\boldsymbol{X}}}, \boldsymbol{\sigma}, \boldsymbol{Y}) + \eta(\dot{\boldsymbol{\varepsilon}}^p, \dot{\boldsymbol{X}}, \overline{\boldsymbol{\sigma}}, \overline{\boldsymbol{Y}}) + \underset{\sim}{\eta}(\overline{\dot{\boldsymbol{\varepsilon}}^p}, \dot{\overline{\boldsymbol{Y}}}, \boldsymbol{\sigma}, \boldsymbol{X}) + \underset{\sim}{\eta}(\dot{\boldsymbol{\varepsilon}}^p, \dot{\boldsymbol{Y}}, \overline{\boldsymbol{\sigma}}, \overline{\boldsymbol{X}})\,\mathrm{d}\Omega\,\mathrm{d}t$$
$$+\frac{1}{2}\int_\Omega \mathrm{Tr}[\mathbf{K}^{-1}(\boldsymbol{\sigma}-\overline{\boldsymbol{\sigma}})(\boldsymbol{\sigma}-\overline{\boldsymbol{\sigma}})] + (\boldsymbol{Y}-\overline{\boldsymbol{Y}})\circ(\boldsymbol{X}-\overline{\boldsymbol{X}})\,\mathrm{d}\Omega\Big|_T$$

The last term is positive due to the convexity of the $\boldsymbol{X} \to \psi_p(\boldsymbol{X})$ part of the free energy. The absolute error is here defined as

$$\underset{\sim}{e} \equiv \frac{1}{2}\int_0^T \int_\Omega \underset{\sim}{\eta}(\dot{\boldsymbol{\varepsilon}}^p, \dot{\boldsymbol{X}}, \boldsymbol{\sigma}, \boldsymbol{Y}) + \underset{\sim}{\eta}(\dot{\boldsymbol{\varepsilon}}^p, \dot{\boldsymbol{Y}}, \boldsymbol{\sigma}, \boldsymbol{X})\, \mathrm{d}\Omega\, \mathrm{d}t \tag{30}$$

where

$$\underset{\sim}{\eta}(\dot{\boldsymbol{\varepsilon}}^p, \dot{\boldsymbol{Y}}, \boldsymbol{\sigma}, \boldsymbol{X}) = \underset{\sim}{\varphi}(\dot{\boldsymbol{\varepsilon}}^p, -\dot{\boldsymbol{Y}}) + \underset{\sim}{\varphi}^*(\boldsymbol{\sigma}, \boldsymbol{X}) - \mathrm{Tr}[\boldsymbol{\sigma}\dot{\boldsymbol{\varepsilon}}^p] + \boldsymbol{X} \circ \dot{\boldsymbol{Y}} \tag{31}$$

$\underset{\sim}{\varphi}^*(\boldsymbol{\sigma}, \boldsymbol{X}) = \varphi^*(\boldsymbol{\sigma}, \mathbf{G}(\boldsymbol{X}))$ and $\underset{\sim}{\varphi}(\dot{\boldsymbol{\varepsilon}}^p, -\dot{\boldsymbol{Y}})$ is the dual potential of $\underset{\sim}{\varphi}^*(\boldsymbol{\sigma}, \boldsymbol{X})$.

### *3.4. Error measurement for a model with bipotential*

According to the properties satisfied by the bipotential, we propose defining the error as

$$\eta(\dot{\boldsymbol{\varepsilon}}^p, \dot{\boldsymbol{X}}, \boldsymbol{\sigma}, \boldsymbol{Y}) = b([\dot{\boldsymbol{\varepsilon}}^p, -\dot{\boldsymbol{X}}], [\boldsymbol{\sigma}, \boldsymbol{Y}]) - \mathrm{Tr}[\boldsymbol{\sigma}\dot{\boldsymbol{\varepsilon}}^p] + \boldsymbol{Y} \circ \dot{\boldsymbol{X}} \tag{32}$$

An absolute error is obtained using the norm (24). Unfortunately, it seems difficult a priori to obtain in the general case, a link between this error and the gap occuring between the admissible and exact solutions.

### *3.5. Dual potential expressions*

Herein, we provide the expression of dual potentials for the standard normal formulations presented previously. The dual potential is calculated analytically from the expression (20). $\underset{\sim}{R}$ and $\underset{\sim}{p}$ have been replaced by $R$ and $p$ for the simplicity of notation. $\Psi_A$ is the indicator function associated with the convex domain $A$; $z$ stands for $\|\boldsymbol{\sigma}^D\| - (R + R_0)$ in the linear hardening case and $\|\boldsymbol{\sigma}^D\| - (1/(\alpha+1))R^{\alpha+1} + R_0)$ in the power hardening case; $\alpha, \alpha'$ and $n, n'$ are linked by $\alpha\alpha' = 1$ and $nn' = 1$, and finally:

$$C_1^* = \{(\boldsymbol{\sigma}, R) \in \mathbf{f} \mid z \leqslant 0\} \qquad C_1 = \{(\dot{\boldsymbol{\varepsilon}}^p, -\dot{p}) \in \mathbf{e} \mid \mathrm{Tr}[\dot{\boldsymbol{\varepsilon}}^p] = 0\}$$
$$C_2^* = \{(\boldsymbol{\sigma}, R) \in \mathbf{f} \mid R \geqslant 0\} \qquad C_2 = \{(\dot{\boldsymbol{\varepsilon}}^p, -\dot{p}) \in \mathbf{e} \mid \|\dot{\boldsymbol{\varepsilon}}^p\| - \dot{p} \leqslant 0\}$$
$$C_3 = \{(\dot{\boldsymbol{\varepsilon}}^p, -\dot{p}) \in \mathbf{e} \mid -\dot{p} \leqslant 0\}$$

*Prandtl–Reuss plastic model with linear hardening*

$$\varphi^*(\boldsymbol{\sigma}, R) = \Psi_{C_1^*} \qquad \varphi(\dot{\boldsymbol{\varepsilon}}^p, -\dot{p}) = R_0\dot{p} + \Psi_{C_1 \cap C_2} \tag{33}$$

Note that the condition $R \geqslant 0$ may be introduced to the definition of the dissipation potential. This does not change the behavior of the material, but the potentials are now written:

$$\varphi^*(\boldsymbol{\sigma}, R) = \Psi_{C_1^* \cap C_2^*} \qquad \varphi(\dot{\boldsymbol{\varepsilon}}^p, -\dot{p}) = R_0\|\dot{\boldsymbol{\varepsilon}}^p\| + \Psi_{C_1 \cap C_2} \tag{34}$$

For a given admissible solution, the errors measured with the potentials (33) or (34) will not generally coincide. Thus, what potentials should be chosen? The choice of the potentials depends upon the context. Here, in applications, we will use the couple (34), as this choice ensures a continuity in writing the potentials in the power hardening law case. The condition $R \geqslant 0$ is indeed naturally respected in this case.

*Prandtl–Reuss plastic model with power hardening*

$$\varphi^*(\boldsymbol{\sigma}, R) = \Psi_{C_1^* \cap C_2^*}$$
$$\varphi(\dot{\boldsymbol{\varepsilon}}^p, -\dot{p}) = R_0\|\dot{\boldsymbol{\varepsilon}}^p\| - \frac{1}{\alpha'+1}\left(\frac{\dot{p}}{\|\dot{\boldsymbol{\varepsilon}}^p\|}\right)^{\alpha'+1}\|\dot{\boldsymbol{\varepsilon}}^p\| + \Psi_{C_1 \cap C_3}$$

*Viscoplastic model with linear hardening*

$$\varphi^*(\boldsymbol{\sigma}, R) = \frac{k}{n+1}\langle z\rangle_+^{n+1} + \Psi_{C_2^*}$$

$$\varphi(\dot{\boldsymbol{\varepsilon}}^p, -\dot{p}) = R_0\|\dot{\boldsymbol{\varepsilon}}^p\| + \frac{k}{n'+1}\left(\frac{\|\dot{\boldsymbol{\varepsilon}}^p\|}{k}\right)^{n'+1} + \Psi_{C_1\cap C_2}$$

*Viscoplastic model with power hardening*

$$\varphi^*(\boldsymbol{\sigma}, R) = \frac{k}{n+1}\langle z\rangle_+^{n+1} + \Psi_{C_2^*}$$

$$\varphi(\dot{\boldsymbol{\varepsilon}}^p, -\dot{p}) = R_0\|\dot{\boldsymbol{\varepsilon}}^p\| + \frac{k}{n'+1}\left(\frac{\|\dot{\boldsymbol{\varepsilon}}^p\|}{k}\right)^{n'+1} - \frac{1}{\alpha'+1}\left(\frac{\dot{p}}{\|\dot{\boldsymbol{\varepsilon}}^p\|}\right)^{\alpha'+1}\|\dot{\boldsymbol{\varepsilon}}^p\| + \Psi_{C_1\cap C_3}$$

The regularization of the plastic potential $\varphi^*$, as we move to viscoplasticity, and of the linear hardening potential $\varphi$, as we move to power hardening may be observed.

## 4. Finite element and admissible solutions

The dissipation error cannot be directly measured on the finite element solution because it is not generally admissible. We will now see how it is possible to easily get an admissible solution from the finite element one in the case of the classical incremental finite element computation obtained through the displacement method. But, let us first detail the discrete problem.

### *4.1. The discrete problem*

In an incremental method, the problem to be solved on $[0, T]$ is divided into a succession of resolutions over $[t_n, t_{n+1}]$ $(n = 0, \ldots, N-1;\ t_0 = 0;\ t_N = T)$. Assuming the solution is known up until the time instant $t_n$, one must then build the solution over $[t_n, t_{n+1}]$. First, a time discretization must be carried out. Usually, one only searches the solution at the final time $t_{n+1}$. So, the kinematic constraints and the equilibrium equation are written at $t_{n+1}$, and the behavior becomes a nonlinear algebraic relation linking the fields at $t_{n+1}$. Formally:

$$\boldsymbol{\sigma}_{n+1} - \boldsymbol{\sigma}_n = \mathscr{A}_n(\boldsymbol{\varepsilon}_{n+1} - \boldsymbol{\varepsilon}_n) \tag{35}$$

where $\boldsymbol{\sigma}_n$, $\boldsymbol{\varepsilon}_n$ and $\boldsymbol{\sigma}_{n+1}$, $\boldsymbol{\varepsilon}_{n+1}$ are the stresses and strains at the times $t_n$ and $t_{n+1}$, respectively. The $\mathscr{A}_n$ notation recalls that the stress at $t_{n+1}$ is no longer expressed as a functional law of the strain rate history, but now as a nonlinear algebraic law of the increase of strain $\boldsymbol{\varepsilon}_{n+1} - \boldsymbol{\varepsilon}_n$ over the time step. Note that if the behavior is described by internal variables, they will, in general, explicitly appear in the numerical scheme.

Concerning the space discretization, it is the displacement formulation (1, 4) that is commonly discretized. The domain is divided into elements on which the displacement field is interpolated between nodal values using simple functions called shape functions. The displacement at $\underline{M}$ reads

$$\underline{U_h(M)} = \mathbf{N}(\underline{M})\mathbf{q} \tag{36}$$

where $\mathbf{N}(\underline{M})$ is the shape function matrix and $\mathbf{q}$ the nodal displacement set. $\mathscr{U}_h$ denotes the finite element displacement space and $\mathscr{S}_h$ the space of stresses defined at the integration points of the domain $\Omega$. The extensions of these two spaces to the whole time interval are denoted $\mathscr{U}_h^{[0,T]}$ and $\mathscr{S}_h^{[0,T]}$. We are now able to write the discrete problem to be solved at $t_{n+1}$:

*The kinematic constraints*

$$\underline{U}_{h,n+1} \in \mathscr{U}_{h,\mathrm{ad}}^{t_{n+1}} \tag{37}$$

where

$$\mathscr{U}_{h,\mathrm{ad}}^{t_{n+1}} = \{\underline{U} \in \mathscr{U}_h \text{ such that } \underline{U} = \underline{U}_d \text{ on } \partial_1\Omega \text{ at } t_{n+1}\} \tag{38}$$

Let us also define $\mathscr{U}_{h,0}$:

$$\mathcal{U}_{h,0} = \{\underline{U} \in \mathcal{U}_h \text{ such that } \underline{U} = 0 \text{ on } \partial_1 \Omega\} \tag{39}$$

*The static equilibrium equations*

$$\boldsymbol{\sigma}_{h,n+1} \in \mathcal{S}_{h,\text{ad}}^{t_{n+1}} \tag{40}$$

where

$$\mathcal{S}_{h,\text{ad}}^{t_{n+1}} = \{\boldsymbol{\sigma} \in \mathcal{S}_h \text{ satisfying (41) at } t_{n+1} \ \forall \underline{U}^* \in \mathcal{U}_{h,0}\}$$

$$\int_{\Omega_h} \text{Tr}[\boldsymbol{\sigma}\boldsymbol{\varepsilon}(\underline{U}^*)] \, \text{d}\Omega_h - \int_{\Omega} \underline{f}_d \circ \underline{U}^* \, \text{d}\Omega - \int_{\partial_2 \Omega} \underline{F}_d \circ \underline{U}^* \, \text{d}S = 0 \tag{41}$$

*The behavior*

$$\boldsymbol{\sigma}_{h,n+1} - \boldsymbol{\sigma}_{h,n} = \mathcal{A}_n(\boldsymbol{\varepsilon}(\underline{U}_{h,n+1}) - \boldsymbol{\varepsilon}(\underline{U}_{h,n})) \tag{42}$$

The integration $\int_{\Omega_h} \cdot \, \text{d}\Omega_h$ in (41) is classically done using a discrete integration technique. An exact analytical integration is indeed not possible due to the nonlinearities present in the behavior. Thus, the stresses given by the computation (as well as the plastic strains and internal variables) are only known at the integration points.

Eqs. (37), (40) and (42) form a nonlinear algebraic system. This system is solved in an iterative way, typically with Newton's method. Two types of solutions always exist as the iterations proceed: a solution $(\check{\underline{U}}_{h,n+1}, \check{\boldsymbol{\sigma}}_{h,n+1})$ satisfying both the kinematic constraints and the equilibrium in a finite element sense:

$$\check{\underline{U}}_{h,n+1} \in \mathcal{U}_{h,\text{ad}}^{t_{n+1}} \qquad \check{\boldsymbol{\sigma}}_{h,n+1} \in \mathcal{S}_{h,\text{ad}}^{t_{n+1}} \tag{43}$$

and a solution $(\tilde{\underline{U}}_{h,n+1}, \tilde{\boldsymbol{\sigma}}_{h,n+1})$ satisfying both the kinematic constraints and the 'discrete' behavior:

$$\tilde{\underline{U}}_{h,n+1} \in \mathcal{U}_{h,\text{ad}}^{t_{n+1}} \qquad \tilde{\boldsymbol{\sigma}}_{h,n+1} - \tilde{\boldsymbol{\sigma}}_{h,n} = \mathcal{A}_n(\boldsymbol{\varepsilon}(\tilde{\underline{U}}_{h,n+1}) - \boldsymbol{\varepsilon}(\tilde{\underline{U}}_{h,n})) \tag{44}$$

Classically, deriving a solution $(\tilde{\underline{U}}_{h,n+1}, \tilde{\boldsymbol{\sigma}}_{h,n+1})$ from the solution $(\check{\underline{U}}_{h,n+1}, \check{\boldsymbol{\sigma}}_{h,n+1})$ ('behavior phase') is performed by integrating the behavior at each integration point of the structure with $\tilde{\underline{U}}_{h,n+1} = \check{\underline{U}}_{h,n+1}$. Deriving a solution $(\check{\underline{U}}_{h,n+1}, \check{\boldsymbol{\sigma}}_{h,n+1})$ from $(\tilde{\underline{U}}_{h,n+1}, \tilde{\boldsymbol{\sigma}}_{h,n+1})$ ('equilibrium phase') is performed by a linear global resolution. When the two types of solutions are close to one another, the iterative process stops and the code generally gives the solution satisfying the 'discrete' behavior.

### *4.2. The construction of an admissible solution*

From the finite element solution, we must construct an admissible solution (denoted by hats), i.e. satisfying:

$$\hat{\underline{U}} \in \mathcal{U}_{\text{ad}}^{[0,T]} \qquad \hat{\boldsymbol{\sigma}} \in \mathcal{S}_{\text{ad}}^{[0,T]}$$

$$\hat{\boldsymbol{\sigma}} = \mathbf{K}(\boldsymbol{\varepsilon}(\hat{\underline{U}}) - \hat{\boldsymbol{\varepsilon}}^p) \qquad \hat{Y} = \mathbf{G}(\hat{X}) \quad \text{on } [0, T] \times \Omega$$

$$(\hat{\boldsymbol{\varepsilon}}^p, \hat{X}) = 0 \quad \text{at } t = 0 \text{ on } \Omega$$

Depending on the type of model, an admissible solution will not necessarily lead to a bounded error. For instance, for models such that the plasticity or viscoplasticity takes place at a constant volume, i.e. $\text{Tr}[\dot{\boldsymbol{\varepsilon}}^p] = 0$, the error will be $+\infty$ if $\text{Tr}[\hat{\dot{\boldsymbol{\varepsilon}}}^p] \neq 0$ (whether we are working with a standard normal, bistandard or even a non-standard bipotential formulation). So, among the admissible solutions, we will only consider the ones leading to a finite error.

The rather unrestrictive assumption of linear evolution for imposed loads and displacements between consecutive computed time is applied. We also assume that the prescribed displacements and applied loads are zero at $t = 0$.

#### *4.2.1. Construction of* $\hat{\boldsymbol{\sigma}} \in \mathcal{S}_{\text{ad}}^{[0,T]}$

The finite element stresses are not statically admissible at the time steps (they are not even known at every point, but only at the integration points). Let us first construct rigorously equilibrated stresses at each time step.

Suppose we do have stresses that satisfy the equilibrium equation in the finite element sense $\check{\boldsymbol{\sigma}}_{h,n+1}$ (if this is

not the case, we just need to apply the 'equilibrium phase' of the iterative method). From these stresses, we then construct the rigorously-equilibrated stresses using techniques developed for the elasticity [3]. These techniques consist first of building load densities in equilibrium with the applied loading on the boundary of each element. Then, stresses are built on each element separately. The density-building only requires the resolution of small linear local problems, and the stress-building is conducted analytically element by element.

With equilibrated stresses at each time step at our disposal and owing to the linear evolution of the loading, we interpolate them over each time step to obtain $\hat{\boldsymbol{\sigma}} \in \mathscr{S}_{\text{ad}}^{[0,T]}$. Let $a_n$ and $a_{n+1}$ be the values of $a$ at $t_n$ and $t_{n+1}$, respectively,. Linear interpolation of $a$ means

$$\text{on} \quad [t_n, t_{n+1}] \quad a = \frac{t_{n+1} - t}{t_{n+1} - t_n} a_n + \frac{t - t_n}{t_{n+1} - t_n} a_{n+1} \tag{45}$$

At $t = 0$, we take $\hat{\boldsymbol{\sigma}}_{h,0} = 0$, which is statically admissible with the initial null loading.

*4.2.2. Construction of* $\hat{\underline{U}} \in \mathscr{U}_{\text{ad}}^{[0,T]}$

Since the prescribed displacements display linear evolution on each time step and since the finite element displacement field satisfies the kinematic constraints at each computer time, an element of $\mathscr{U}_{\text{ad}}^{[0,T]}$ is simply obtained by interpolating the finite element displacement field between the computed times. At $t = 0$, we take $\hat{\underline{U}} = 0$, which is kinematically admissible with the initial prescribed null displacement. If the inelastic strains occur at constant volume, the finite element field must be modified at each computed time before the interpolation in order to fulfill the incompressibility condition $\text{Tr}[\boldsymbol{\varepsilon}(\hat{\underline{U}}) - \mathbf{K}^{-1}\hat{\boldsymbol{\sigma}}] = 0$. This modification can be achieved and is inspired by previous work for incompressible and quasi-incompressible elasticity [32]. It will be the subject of a forthcoming paper. For the plane stress problems treated in the application, the condition $\text{Tr}[\boldsymbol{\varepsilon}(\hat{\underline{U}}) - \mathbf{K}^{-1}\hat{\boldsymbol{\sigma}}] = 0$ can be achieved easily.

*4.2.3. Construction of the inelastic strains*

The following expression must be used to compute the inelastic strains on $[0, T] \times \Omega$ in order to respect Hooke's law:

$$\hat{\boldsymbol{\varepsilon}}^p = \boldsymbol{\varepsilon}(\hat{\underline{U}}) - \mathbf{K}^{-1}\hat{\boldsymbol{\sigma}} \tag{46}$$

As $\hat{\underline{U}} = 0$ and $\hat{\boldsymbol{\sigma}} = 0$ at $t = 0$ on $\Omega$, we have $\hat{\boldsymbol{\varepsilon}}^p = 0$ at $t = 0$ on $\Omega$. We thus satisfy the initial condition on $\hat{\boldsymbol{\varepsilon}}^p$.

*4.2.4. Construction of the internal variables*

The computed internal variables are seldom given in classical finite element code. Herein, we do not consider them given at the computed time, and we construct them. Several choices are possible. We may, for instance, build them in order to minimize the error or in order to be as close as possible to the numerical integration scheme used in the computation. Let us consider these two cases.

*Error minimization*

As the behavior of the material is local in space, the minimization is carried out independently at each point of the structure. $\mathbf{X}^{[0,T]}$ denotes the space where the internal variables defined on $[0, T]$ are to be found. The minimization problem at a given point of the structure reads

$$\min_{\hat{\boldsymbol{\chi}} \in \mathbf{X}^{[0,T]}} \int_0^T \eta \, \mathrm{d}t$$

with

$$\hat{\boldsymbol{Y}} = \mathbf{G}(\hat{\boldsymbol{X}}) \quad \text{and} \quad \hat{\boldsymbol{X}} = 0 \quad \text{at } t = 0$$

The expression of $\eta$ depends upon the model considered. The variables $\hat{\boldsymbol{\sigma}}$ and $\hat{\boldsymbol{\varepsilon}}$ have been built at each time step, and then interpolated between these times. We will follow the same path to build the internal variables. In order to limit costs, this building process will be incremental. Suppose the internal variables are known up until

$t_n$ at a point, the internal variables at $t_{n+1}$ will be obtained at the same point by solving the following local problem:

$$\min_{\hat{X}_{n+1}\in X^{t_{n+1}}} \int_{t_n}^{t_{n+1}} \eta \, dt \tag{47}$$

with

$$\hat{Y} = \mathbf{G}(\hat{X}) \quad \text{and} \quad \hat{X} = \frac{t_{n+1}-t}{t_{n+1}-t_n}\hat{X}_n + \frac{t-t_n}{t_{n+1}-t_n}\hat{X}_{n+1}$$

$\mathbf{X}^{t_{n+1}}$ denotes the space where the internal variables defined at $t_{n+1}$ are to be found. In order to explicitly express (47) in terms of the unknown $\hat{X}_{n+1}$, an approximate integration can be performed.

We now focus on the case of a normal standard formulation. On $[t_n, t_{n+1}]$, $\dot{X}$ and $\dot{\varepsilon}^p$ are constants and $\eta$ depends on times only through $\hat{\sigma}$ and $\hat{Y}$. Using the trapezoidal integration rule to approximate (47), one gets

$$\min_{\hat{X}_{n+1}\in \mathbf{X}^{t_{n+1}}} \frac{t_{n+1}-t_n}{2}\left(\eta(\hat{\varepsilon}^p_{n+1}, \hat{X}_{n+1}, \hat{\sigma}_n, \hat{Y}_n) + \eta(\hat{\varepsilon}^p_{n+1}, \hat{X}_{n+1}, \hat{\sigma}_{n+1}, \hat{Y}_{n+1})\right) \tag{48}$$

with

$$\hat{Y}_{n+1} = \Lambda \hat{X}_{n+1}, \qquad \hat{\varepsilon}^p_{n+1} = \frac{(\hat{\varepsilon}^p_{n+1} - \hat{\varepsilon}^p_n)}{t_{n+1}-t_n}, \qquad \hat{X}_{n+1} = \frac{(\hat{X}_{n+1} - \hat{X}_n)}{t_{n+1}-t_n}$$

The goal function of this minimization problem is strictly convex with respect to $\hat{X}_{n+1}$. Thus, the solution will be unique. Also, note that owing to the convexity of $\eta$ with respect to the variables $(\sigma, Y)$, the expression (48) always overestimates the exact expression (47). In the particular case of plasticity, both expressions are equivalent.

*Numerical scheme*

We consider the models described in Section 3.5. Suppose the internal variable $\hat{p}$ is known up until $t_n$ at a point, the internal variable at $t_{n+1}$ will be obtained at the same point by $\hat{p}_{n+1} = \sup(\hat{p}_{1,n+1}, \hat{p}_{2,n+1})$ where $\hat{p}_{1,n+1}$ and $\hat{p}_{2,n+1}$ depends on the model considered. For the Prandtl–Reuss plastic model with linear hardening $\hat{p}_{1,n+1}$ and $\hat{p}_{2,n+1}$ are given by

$$\hat{p}_{1,n+1} = \hat{p}_n + (t_{n+1}-t_n)\|\hat{\dot{\varepsilon}}^p_{n+1}\|$$

$$\hat{p}_{2,n+1} = \frac{1}{\lambda}\langle\|\hat{\sigma}^D_{n+1}\| - R_0\rangle_+$$

For the Prandtl–Reuss plastic model with power hardening:

$$\hat{p}_{1,n+1} = \hat{p}_n + (t_{n+1}-t_n)\|\hat{\dot{\varepsilon}}^p_{n+1}\| l'(\lambda \hat{p}_{1,n+1})$$

$$\hat{p}_{2,n+1} = \frac{1}{\lambda} l^{-1}(\langle\|\hat{\sigma}^D_{n+1}\| - R_0\rangle_+)$$

For the viscoplastic model with linear hardening:

$$\hat{p}_{1,n+1} = \hat{p}_n + (t_{n+1}-t_n)\|\hat{\dot{\varepsilon}}^p_{n+1}\|$$

$$\hat{p}_{2,n+1} = \frac{1}{\lambda}\left\langle\|\hat{\sigma}^D_{n+1}\| - R_0 - \left(\frac{\|\hat{\dot{\varepsilon}}^p_{n+1}\|}{k}\right)^{1/n}\right\rangle_+$$

For the viscoplastic model with power hardening:

$$\hat{p}_{1,n+1} = \hat{p}_n + (t_{n+1}-t_n)\|\hat{\dot{\varepsilon}}^p_{n+1}\| l'(\lambda \hat{p}_{1,n+1})$$

$$\hat{p}_{2,n+1} = \frac{1}{\lambda} l^{-1}\left(\left\langle\|\hat{\sigma}^D_{n+1}\| - R_0 - \left(\frac{\|\hat{\dot{\varepsilon}}^p_{n+1}\|}{k}\right)^{1/n}\right\rangle_+\right)$$

where $l(R) = 1/(\alpha+1)R^{\alpha+1}$. These relations are inspired by the numerical implicit scheme used in the

computation. In the applications, we will use this second approach to build the internal variables instead of minimizing the error. In fact, the results obtained by the two approaches are quite similar and in the particular case of the plastic model with linear hardening, they are identical.

## 5. Examples of dissipation error estimation

We will consider plane stress problems. The incompressibility condition for the inelastic strains is satisfied by adequately choosing the strain in the width ($\hat{\varepsilon}_{33}$). The finite element solutions are obtained by the code CASTEM2000. Triangular elements with three and six nodes are used. All examples were treated dimensionalessly.

### *5.1. First example: The holed plate problem*

A loading (Fig. 1), followed by an unloading, is applied to the extremity of a square plate with a square hole. Owing to the symmetry, only a quarter of the problem is considered (Fig. 2). The Prandtl–Reuss plastic model with linear hardening and the following dimensionless parameters is used.

$$R_0 = 1\,, \quad k_y = 8.16\,, \quad E = 244.95\,, \quad \nu = 0.3$$

$E$ and $\nu$ denote Young's modulus and Poisson's ratio, respectively. The finite element computation is performed with 42 six-node triangular elements (Fig. 3) and eight equal time increments. The final hardening threshold level is given in Fig. 4. The dissipation error is 14.71%. Figs. 5–7 highlight each element contribution, the evolution in time of the contribution to the error and each time step contribution, respectively.

### *5.2. Second example: The frame problem*

A frame (Fig. 8) is submitted to a growing, then deceasing load on its right side (thin line in Fig. 9). Then, an increasing pressure is applied to its upper part (thick line in Fig. 9). The Prandtl–Reuss plastic model with linear hardening is again considered. The finite element computation is carried out with 352 three-node triangles (Fig. 10) and 12 time increments (8 for the pressure on the right side, and 4 for the upper side). The threshold levels obtained at $t = 2$ and $t = 4$ are given in Figs. 11 and 12, respectively. The dissipation error is 35.97%. Figs.

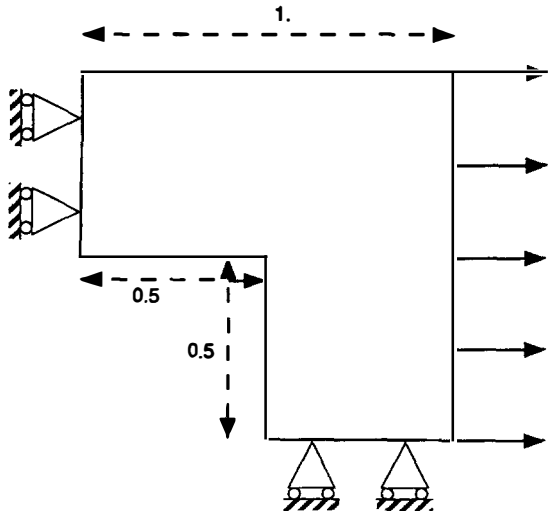


Fig. 1. The loading.

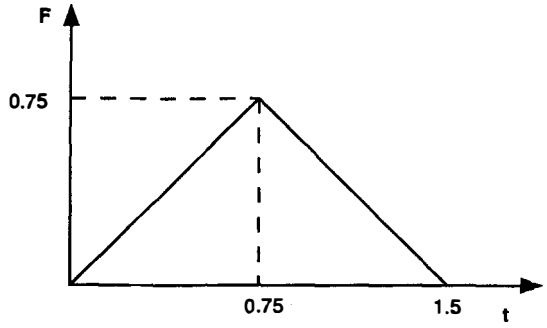


Fig. 2. The holed plate problem.

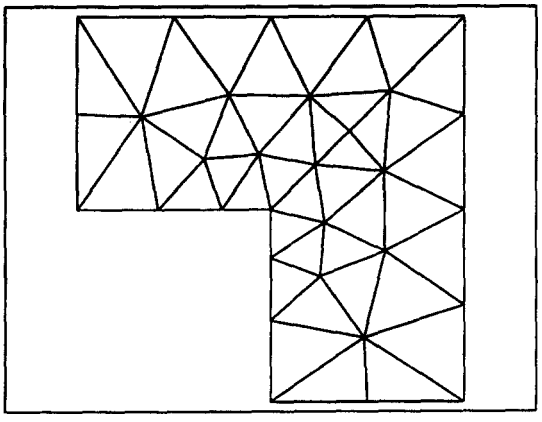

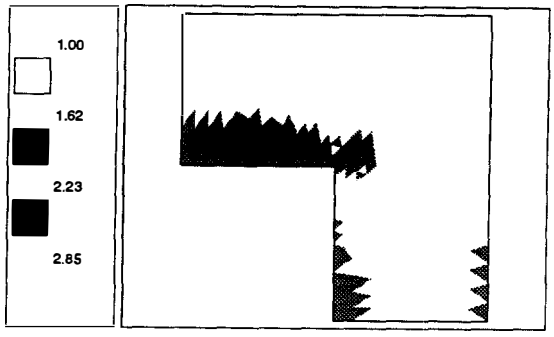


Fig. 3. The mesh: 42 six-node triangles and 103 nodes.

Fig. 4. Final hardening threshold; initial threshold: $R_0 = 1$.

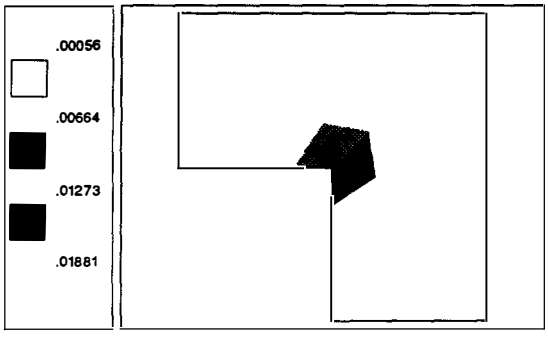


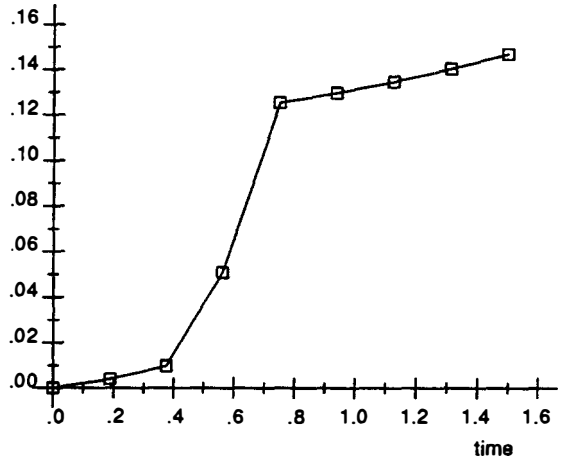


Fig. 5. Contribution of each element to the error.

Fig. 6. The evolution of the contribution to the error vs. time (see Eq. (29)).

13–15 show each element contribution, and evolution in time of the contribution to the error and each time step contribution, respectively.

### *5.3. Third example: The square plate problem*

Consider a square plate loaded on its right side under uniform tension. A uniform body force places this tension in equilibrium. Owing to the symmetry, only the upper-half part of the plate will be studied (Fig. 16). The loading evolves monotonically (Fig. 17). The viscoplastic version of the Prandtl–Reuss plastic model with linear hardening is used. The dimensionless material parameters are:

$$R_0 = 0.7\,, \quad k_y = 8.16\,, \quad E = 244.95\,, \quad \nu = 0.3\,, \quad n = 2\,, \quad k = 2.25$$

The mesh (Fig. 18) contains 16 three-node triangular elements. The plastic computation is carried out with four identical time increments. The plastic threshold obtained at the final time is given in Fig. 19. The error dissipation is 21.30% for this computation. Figs. 20–22 display each element contribution, the evolution in time of the contribution to the error and each time step contribution, respectively. The last time step, on which the viscoplastic zone is the largest, contribute the most to the error. Concerning the space, the right part of the plate, where viscoplasticity occurs, contributes more to the error than the left one.

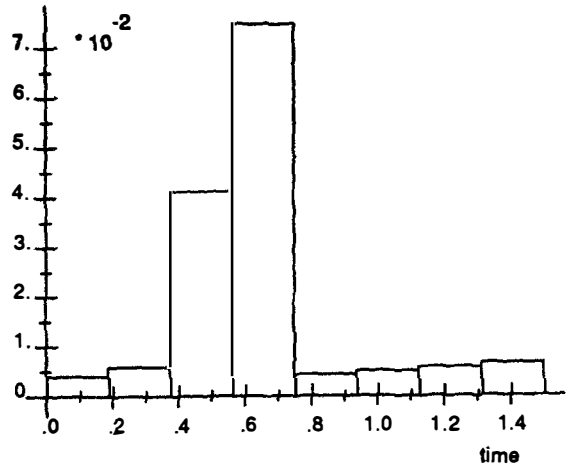


Fig. 7. Contribution of each time increment to the error.

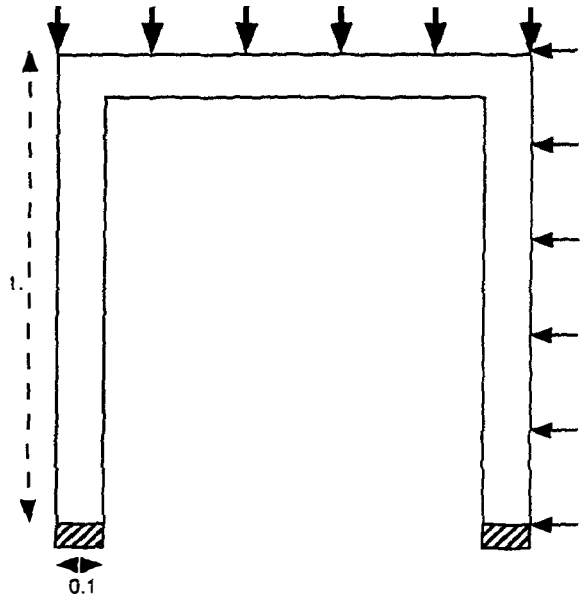


Fig. 8. The frame problem.

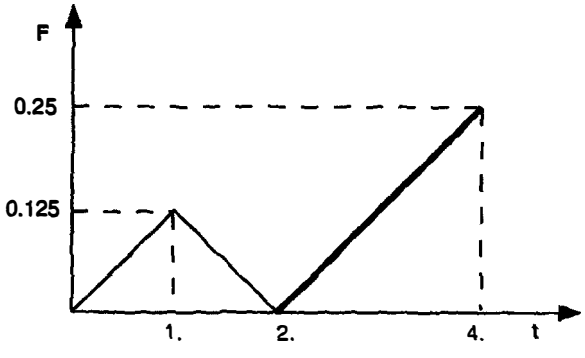


Fig. 9. The loading (thin line for the right side and thick line for the upper part).

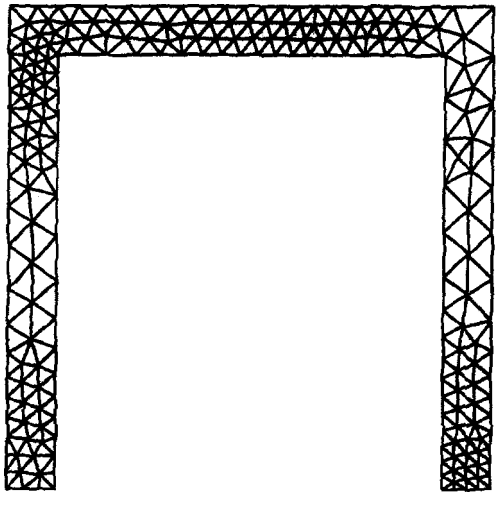

Fig. 10. The mesh: 352 three-node triangles and 235 nodes.

### *5.4. Fourth example: The particular case of an elastic computation*

Consider a (visco)plastic problem for which the exact solution is elastic, i.e. a problem with no singularity and a small loading. The finite element computation for this problem with a single time step leads (if the stresses are all below the yielding stress) to a solution satisfying:

$$\underline{\check{U}}_h = \underline{\tilde{U}}_h \qquad \check{\boldsymbol{\sigma}}_h = \tilde{\boldsymbol{\sigma}}_h = \mathbf{K}\boldsymbol{\varepsilon}(\underline{\tilde{U}}_h)$$

This solution is not admissible since the field stress $\check{\boldsymbol{\sigma}}_h$ does not exactly satisfy the equilibrium equations. The construction of an admissible solution will, is general, yield a non-zero inelastic strain $\hat{\boldsymbol{\varepsilon}}^p$, thereby leading to a non-zero error.

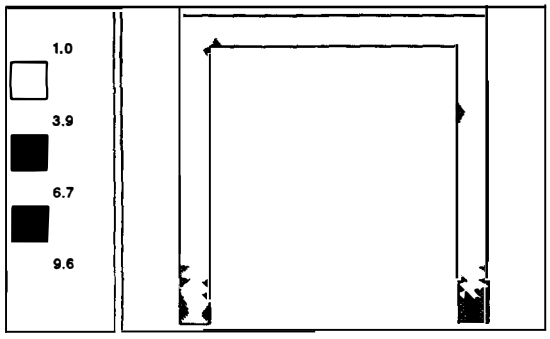


Fig. 11. Hardening threshold at the end of the first loading; initial threshold: $R_0 = 1$.

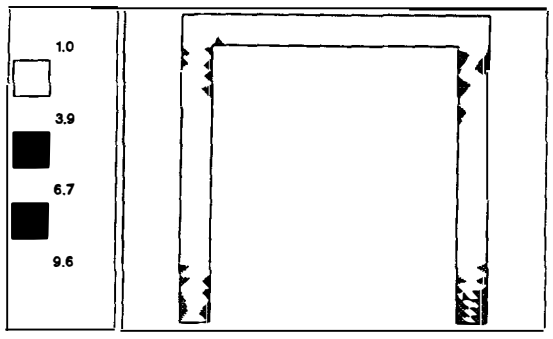


Fig. 12. Final hardening threshold.

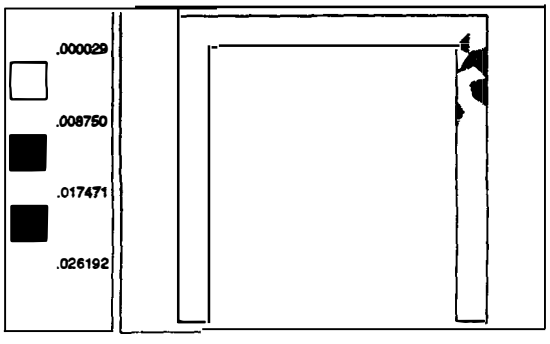


Fig. 13. Contribution of each element to the error.

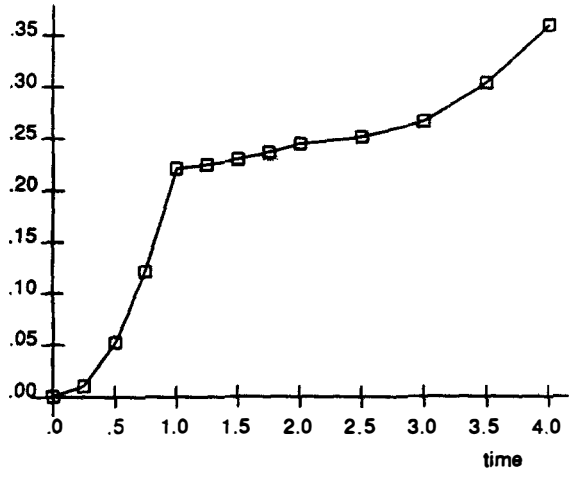


Fig. 14. The evolution of the contribution to the error vs. time (see Eq. (29)).

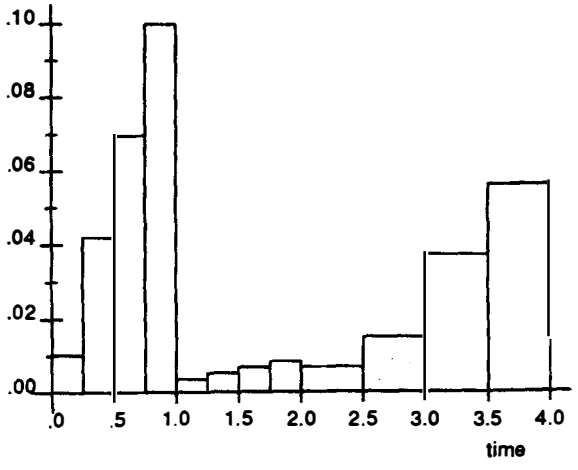


Fig. 15. Contribution of each time step to the error.

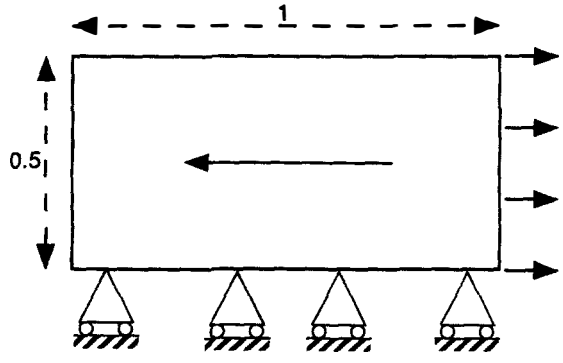


Fig. 16. The square plate problem.

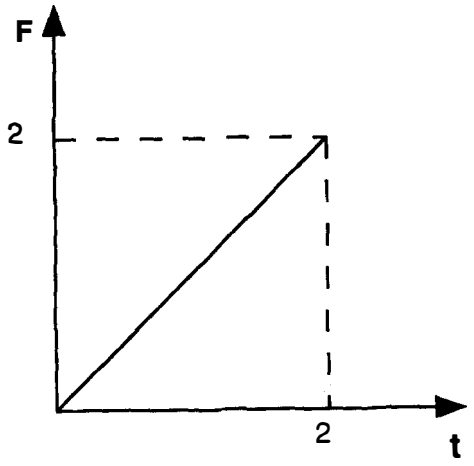


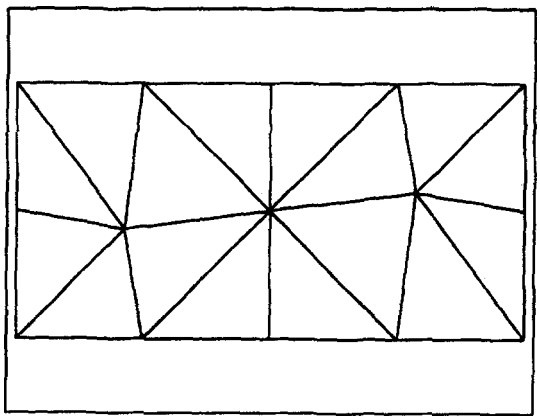

Fig. 17. The monotonous loading.

Fig. 18. The mesh: 16 three-node triangles and 15 nodes.

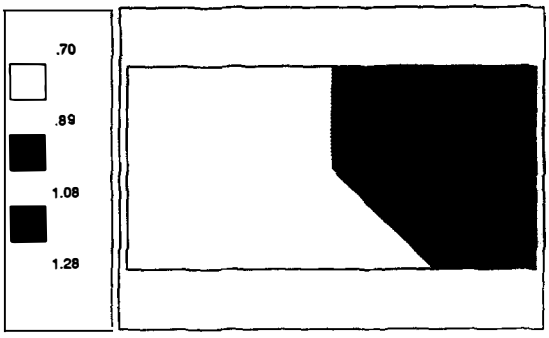


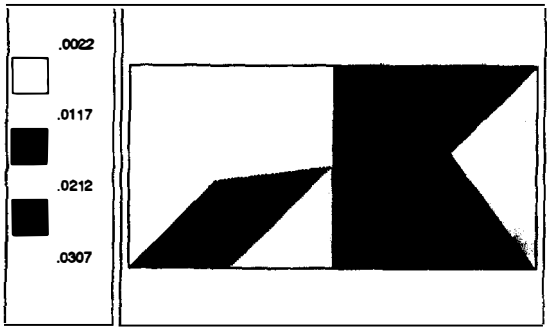


Fig. 19. Final hardening threshold; initial hardening threshold: $R_0 = 0.7$.

Fig. 20. Contribution of each element to the error.

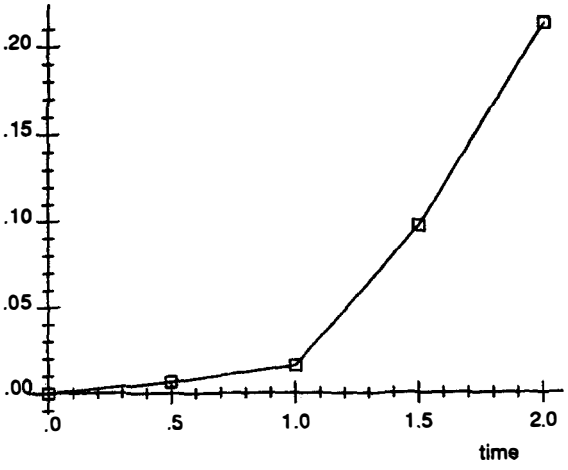


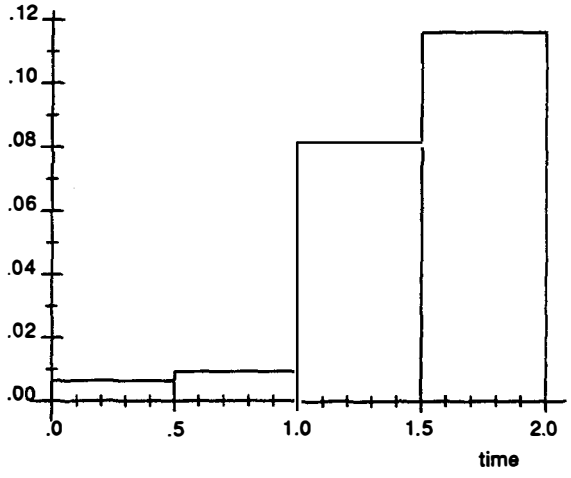


Fig. 21. The evolution of the contribution to the error vs. time (see Eq. (29)).

Fig. 22. Contribution of each time step to the error.

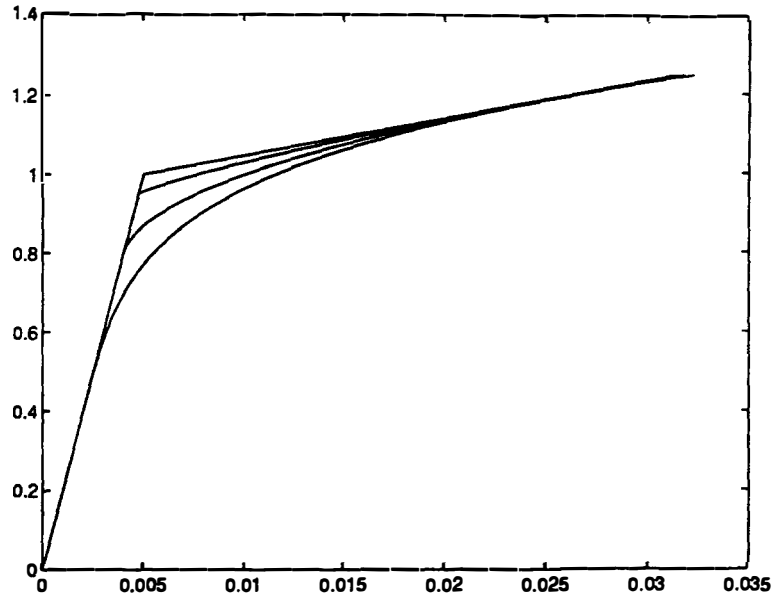


Fig. 23. Equivalent stress–strain relation for the four materials M1, M2, M3, M4 ordered from the bottom to the top.

As an example, consider the square plate problem with a small loading so that the plate stays in an elastic state. The dissipation error is 11.06%. Note that the classical elastic error [3] obtained for the same problem is 12.11%. So, the two errors are similar.

### *5.5. Fifth example: Influence of the hardening law on the error*

We consider four different plastic material M1, M2, M3, M4. Fig. 23 gives the stress–strain relation for the tensile test and Table 1 the dimensionless parameters used. $m$ denotes the power used in the power hardening law. In each case, the elasticity parameters are the same ($E = 244.95$, $\nu = 0.3$).

The dissipation errors obtained with these materials for the square plate problem are given in Table 1. Four time steps are used and several meshes are considered. We can observe that the errors are quite close for the different materials.

Let us now compare the dissipation error $\epsilon$ with the classical free energy norm exact error $\zeta$ defined by

$$\zeta^2 = \frac{\sup_{t\in[0,T]} (\|\boldsymbol{\sigma}_h - \overline{\boldsymbol{\sigma}}\|^2_{\mathbf{K}^{-1}} + \|\boldsymbol{Y}_h - \overline{\boldsymbol{Y}}\|^2_{\boldsymbol{\Lambda}^{-1}})}{\sup_{t\in[0,T]} (\|\boldsymbol{\sigma}_h + \overline{\boldsymbol{\sigma}}\|^2_{\mathbf{K}^{-1}} + \|\boldsymbol{Y}_h + \overline{\boldsymbol{Y}}\|^2_{\boldsymbol{\Lambda}^{-1}})} \tag{49}$$

where

$$\|\bullet\|^2_{\mathbf{K}^{-1}} = \mathrm{Tr}[\mathbf{K}^{-1}\bullet\bullet] \qquad \|\bullet\|^2_{\boldsymbol{\Lambda}^{-1}} = [\boldsymbol{\Lambda}^{-1}\bullet\circ\bullet]$$

The plate square problem treated with eight time steps and 16 elements gives a dissipation error of 23% for the material M4 and the exact free energy error is 14%. So the dissipation error overestimates the exact one by a 1.6 factor. If the loading is smaller, so that the exact solution is elastic, the factor is 1.9.

Table 1
Values of the dimensionless models parameters for the four plastic materials and dissipation errors obtained with different meshes

| | $m$ | $R_0$ | $k_y$ | Mesh 1 | Mesh 2 | Mesh 3 | Mesh 4 |
|---|---|---|---|---|---|---|---|
| M1 | 4.5 | 0.3 | 2.05 | 28.09 | 23.48 | 13.48 | 8.56 |
| M2 | 2.0 | 0.8 | 2.56 | 24.39 | 18.83 | 11.06 | 6.78 |
| M3 | 1.25 | 0.95 | 4.86 | 23.46 | 17.59 | 10.58 | 6.27 |
| M4 | 1.0 | 1.0 | 8.16 | 22.89 | 17.23 | 10.53 | 6.02 |

## 6. Discretization quality influence and error indicators

### *6.1. Time and space reference errors*

The dissipation error takes into account all the unavoidable error sources entering into the computation of a time-dependent nonlinear problem: the space discretization, the time discretization and the iterative technique used to solve the nonlinear discrete problem. Let us observe the behavior of the error when the space or time discretization is refined (the influence of the non-convergence of the iterate algorithm will not studied in this paper). Table 2 presents the evolution of the error $\epsilon$ with an increasing number of time increments for a given mesh and Table 3 presents the evolution of the error for an increasing quality of the mesh and a given time discretization.

We can conclude that the error decreases as the space or time discretization is refined an tends to stabilize beyond a given level or refinement. This result proves that the error depends upon both the space and time discretizations. Beyond a certain refinement in space (time resp.), the error is stable because it is mainly due to the time (space resp.) discretization.

Let a time (space resp.) discretization be given, $\epsilon_{time}$ ($\epsilon_{space}$ resp.) is defined as the dissipation error due to this discretization only, assuming that no error due to space (time resp.) discretization has been committed. Formally, we have

Table 2
Error, space and time indicators in % for a growing number of time steps

| | | | | | |
|---|---|---|---|---|---|
| *The holed plate problem* | | | | | |
| nb step | 2 | 4 | 8 | 16 | 32 |
| $\epsilon$ | 39.58 | 12.96 | 7.93 | 7.30 | 7.66 |
| $i_{space}$ | 5.20 | 5.40 | 6.04 | 7.08 | 7.78 |
| $i_{time}$ | 37.61 | 8.15 | 2.05 | 0.51 | 0.17 |
| *The frame problem* | | | | | |
| nb step | 3 | 6 | 12 | 24 | 48 |
| $\epsilon$ | 25.75 | 16.37 | 13.83 | 13.76 | 14.01 |
| $i_{space}$ | 10.90 | 11.67 | 12.47 | 13.29 | 13.87 |
| $i_{time}$ | 17.68 | 4.82 | 0.92 | 0.24 | 0.08 |
| *The square plate problem* | | | | | |
| nb step | 1 | 2 | 4 | 8 | 16 |
| $\epsilon$ | 42.25 | 17.62 | 13.96 | 12.76 | 12.57 |
| $i_{space}$ | 10.91 | 11.49 | 12.18 | 12.45 | 12.70 |
| $i_{time}$ | 39.92 | 8.24 | 2.64 | 0.80 | 0.33 |

Table 3
Error, time and space indicators in % for a growing quality of the mesh

| Meshes | Mesh 1 | Mesh 2 | Mesh 3 | Mesh 4 | Mesh 5 |
|---|---|---|---|---|---|
| *The holed plate problem* | | | | | |
| $\epsilon$ | 14.71 | 7.93 | 4.35 | 3.70 | 2.59 |
| $i_{time}$ | 2.15 | 2.04 | 2.08 | 2.08 | 2.11 |
| $i_{space}$ | 12.23 | 6.04 | 2.33 | 1.60 | 0.52 |
| *The frame problem* | | | | | |
| $\epsilon$ | 40.94 | 35.89 | 21.79 | 19.47 | 18.64 |
| $i_{time}$ | 19.29 | 17.93 | 17.66 | 17.65 | 17.65 |
| $i_{space}$ | 34.08 | 26.50 | 5.44 | 2.35 | 1.25 |
| *The square plate problem* | | | | | |
| $\epsilon$ | 24.90 | 17.62 | 12.54 | 9.88 | 8.81 |
| $i_{time}$ | 8.80 | 8.24 | 8.06 | 8.04 | 8.10 |
| $i_{space}$ | 20.20 | 11.49 | 5.26 | 2.05 | 0.76 |

$$\epsilon_{\text{time}} \equiv \lim_{h \to 0} \epsilon \quad \text{and} \quad \epsilon_{\text{space}} \equiv \lim_{\Delta t \to 0} \epsilon \tag{50}$$

$h$ ($\Delta t$ resp.) stands for the quality of the space (time resp.) discretization. $\epsilon_{\text{time}}$ and $\epsilon_{\text{space}}$ are called the time and space reference errors, respectively. $\epsilon_{\text{time}}$ and $\epsilon_{\text{space}}$ are theoretical quantities since it is impossible, in practice, to compute a solution with $h = 0$ or $\Delta t = 0$. For a given finite element computation, let us see how it is possible to approximate these quantities.

Two problems exist between the continuous reference problem and the complete discrete problem: the problem discretized in space only and the problem discretized in time only. The dissipation error concept applied to these two 'new' problems give accurate estimates of the theoretical quantities $\epsilon_{\text{time}}$ and $\epsilon_{\text{space}}$. These estimates will be denoted $i_{\text{time}}$, $i_{\text{space}}$ and are called time the space error *indicator*, respectively. Note that a time error indicator has already been introduced in a similar way for the Drucker error [24].

### *6.2. Space and time indicators associated with a finite element solution*

#### *6.2.1. Time error indicator*

The 'time' problem is:

*The kinematic constraints*:

$$\underline{U}_h \in \mathcal{U}_{\text{ad}}^{[0,T]} \tag{51}$$

$$\mathcal{U}_{h,\text{ad}}^{[0,T]} = \{\underline{U} \in \mathcal{U}^{[0,T]} \text{ such that } \underline{U} = \underline{U}_d \text{ on } [0, T] \times \partial_1 \Omega\} \tag{52}$$

*The equilibrium equations*:

$$\boldsymbol{\sigma}_h \in \mathcal{S}_{h,\text{ad}}^{[0,T]} \tag{53}$$

$$\mathcal{S}_{h,\text{ad}}^{[0,T]} = \{\boldsymbol{\sigma} \in \mathcal{S}_h^{[0,T]} \text{ satisfying (41) } \forall\, \underline{U}^* \in \mathcal{U}_{h,0} \text{ and } \forall\, t \in [0, T]\}$$

$$\mathcal{U}_{h,0} = \{\underline{U} \in \mathcal{U}_h \text{ such that } \underline{U} = 0 \text{ on } \partial_1 \Omega\}$$

*The state laws*:

$$\text{on} \quad [0, T] \times \Omega_h \quad \begin{cases} \boldsymbol{\sigma}_h = \mathbf{K}(\boldsymbol{\varepsilon}(\underline{U}_h) - \boldsymbol{\varepsilon}_h^p) \\ \boldsymbol{Y}_h = \boldsymbol{\Lambda} \boldsymbol{X}_h \end{cases} \tag{54}$$

*The evolution laws*:

$$\text{on} \quad [0, T] \times \Omega_h \qquad \begin{pmatrix} \dot{\boldsymbol{\varepsilon}}_h^p \\ -\boldsymbol{X}_h \end{pmatrix} \in \begin{pmatrix} \partial_{\boldsymbol{\sigma}_h} \varphi^*(\boldsymbol{\sigma}_h, \boldsymbol{Y}_h) \\ \partial_{\boldsymbol{Y}_h} \varphi^*(\boldsymbol{\sigma}_h, \boldsymbol{Y}_h) \end{pmatrix} \tag{55}$$

$$\text{at } t = 0 \text{ on } \Omega_h \qquad \boldsymbol{\varepsilon}_h^p = 0 \quad \boldsymbol{X}_h = 0 \tag{56}$$

The time error indicator is

$$I_{\text{time}} \equiv \int_0^T \int_{\Omega_h} \eta(\hat{\boldsymbol{\varepsilon}}_h^p, \hat{\boldsymbol{X}}_h, \hat{\boldsymbol{\sigma}}_h, \hat{\boldsymbol{Y}}_h)\, \mathrm{d}\Omega_h\, \mathrm{d}t \tag{57}$$

The integration over $\Omega_h$ means that we use the same integration points as those used in the finite element computation. The admissible solution $(\hat{\boldsymbol{\varepsilon}}_h^p, \hat{\boldsymbol{X}}_h, \hat{\boldsymbol{\sigma}}_h, \hat{\boldsymbol{Y}}_h)$ must satisfy (51), (53), (54) and (56). $I_{\text{time}}$ is the absolute time indicator. The relative indicator $i_{\text{time}}$ is defined by $I_{\text{time}} / D_{\text{time}}$ where

$$D_{\text{time}} \equiv 2 \sup_{t \in [0,T]} d_t \tag{58}$$

$$d_t \equiv \int_0^t \int_{\Omega_h} \sup \left[ (\varphi^*(\hat{\boldsymbol{\sigma}}_h, \hat{\boldsymbol{Y}}_h) + \varphi(\hat{\boldsymbol{\varepsilon}}_h^p, \hat{\boldsymbol{X}}_h)), \frac{R_0}{\|\hat{\boldsymbol{\sigma}}_h^D\|} |\dot{\psi}_e(\hat{\boldsymbol{\varepsilon}}_h^p)| \right] \mathrm{d}\Omega_h\, \mathrm{d}t$$

$$+ \int_{\Omega_h} \frac{1}{2} \operatorname{Tr}[\mathbf{K}^{-1} \hat{\boldsymbol{\sigma}}_h \hat{\boldsymbol{\sigma}}_h] + \frac{1}{2} \boldsymbol{\Lambda}^{-1} \hat{\boldsymbol{Y}}_h \circ \hat{\boldsymbol{Y}}_h\, \mathrm{d}\Omega_h \Big|_t \tag{59}$$

*6.2.2. Space error indicator*

$\mathcal{U}^{[0,T]_\Delta}$ will denote the space where the displacements defined on $[0,T]_\Delta \times \Omega$ are to be found, and $\mathcal{S}^{[0,T]_\Delta}$ the space where the stresses also defined on $[0,T]_\Delta \times \Omega$ are to be found. $[0,T]_\Delta$ denotes the set of computed times and the following notation is used:

$$\dot{x}_{n+1} = \frac{x_{n+1} - x_n}{t_{n+1} - t_n} \tag{60}$$

The 'space' problem is:

*The kinematic constraints*

$$\underline{U}_{n+1} \in \mathcal{U}_{\text{ad}}^{[0,T]_\Delta} \tag{61}$$

$$\mathcal{U}_{\text{ad}}^{[0,T]_\Delta} = \{\underline{U} \in \mathcal{U}^{[0,T]_\Delta} \text{ such that } \underline{U} = \underline{U}_d \quad \text{on } [0,T]_\Delta \times \partial_1\Omega\} \tag{62}$$

*The equilibrium equations*

$$\boldsymbol{\sigma}_{n+1} \in \mathcal{S}_{\text{ad}}^{[0,T]_\Delta} \tag{63}$$

$$\mathcal{S}_{\text{ad}}^{[0,T]_\Delta} = \{\boldsymbol{\sigma} \in \mathcal{S}^{[0,T]_\Delta} \text{ satisfy (5) } \forall\, \underline{U}^* \in \mathcal{U}_0 \text{ and } \forall\, t \in [0,T]_\Delta\}$$

*The state laws*:

$$\text{on} \quad [0,T]_\Delta \times \Omega \quad \begin{cases} \boldsymbol{\sigma}_{n+1} = \mathbf{K}(\boldsymbol{\varepsilon}(\underline{U}_{n+1}) - \boldsymbol{\varepsilon}^p_{n+1}) \\ \boldsymbol{Y}_{n+1} = \boldsymbol{\Lambda} \boldsymbol{X}_{n+1} \end{cases} \tag{64}$$

*The evolution laws*:

$$\text{on} \quad [0,T]_\Delta \times \Omega \quad \begin{pmatrix} \dot{\boldsymbol{\varepsilon}}^p_{n+1} \\ -\dot{\boldsymbol{X}}_{n+1} \end{pmatrix} \in \begin{pmatrix} \partial_{\boldsymbol{\sigma}_{n+1}} \varphi^*(\boldsymbol{\sigma}_{n+1}, \boldsymbol{Y}_{n+1}) \\ \partial_{\boldsymbol{Y}_{n+1}} \varphi^*(\boldsymbol{\sigma}_{n+1}, \boldsymbol{Y}_{n+1}) \end{pmatrix} \tag{65}$$

$$\text{on } \Omega \quad \boldsymbol{\varepsilon}^p_0 = 0 \quad \boldsymbol{X}_0 = 0 \tag{66}$$

The space error indicator is

$$I_{\text{space}} \equiv \sum_{n=0}^{N-1} (t_{n+1} - t_n) \int_\Omega \eta(\widehat{\dot{\boldsymbol{\varepsilon}}^p}_{n+1}, \hat{\dot{\boldsymbol{X}}}_{n+1}, \hat{\boldsymbol{\sigma}}_{n+1}, \hat{\boldsymbol{Y}}_{n+1})\, \mathrm{d}\Omega \tag{67}$$

$I_{\text{space}}$ really measures the error associated with the problem (61)–(66) because of the following property that is simply a rewriting of (22) at the particular time $t_{n+1}$.

$$\eta(\dot{\boldsymbol{\varepsilon}}^p_{n+1}, \dot{\boldsymbol{X}}_{n+1}, \boldsymbol{\sigma}_{n+1}, \boldsymbol{Y}_{n+1}) = 0 \quad \Leftrightarrow \quad \begin{pmatrix} \dot{\boldsymbol{\varepsilon}}^p_{n+1} \\ -\dot{\boldsymbol{X}}_{n+1} \end{pmatrix} \in \begin{pmatrix} \partial_{\boldsymbol{\sigma}_{n+1}} \varphi^*(\boldsymbol{\sigma}_{n+1}, \boldsymbol{Y}_{n+1}) \\ \partial_{\boldsymbol{Y}_{n+1}} \varphi^*(\boldsymbol{\sigma}_{n+1}, \boldsymbol{Y}_{n+1}) \end{pmatrix} \tag{68}$$

The admissible solution $(\hat{\boldsymbol{\varepsilon}}^p_{n+1}, \hat{\boldsymbol{X}}_{n+1}, \hat{\boldsymbol{\sigma}}_{n+1}, \hat{\boldsymbol{Y}}_{n+1})$ must satisfy (61), (63), (64) and (66) and is constructed by reusing parts of already described techniques. The relative space indicator $i_{\text{space}}$ is defined by $I_{\text{space}} / D_{\text{space}}$ where

$$D_{\text{space}} \equiv 2 \sup_{k \in \{0,\ldots,N-1\}} d_k \tag{69}$$

$$\begin{aligned} d_k \equiv & \sum_{n=0}^{k} (t_{n+1} - t_n) \int_\Omega \sup \left[ (\varphi^*(\hat{\boldsymbol{\sigma}}_{n+1}, \hat{\boldsymbol{Y}}_{n+1}) + \varphi(\hat{\boldsymbol{\varepsilon}}^p_{n+1}, \hat{\boldsymbol{X}}_{n+1})), \frac{R_0}{\|\hat{\boldsymbol{\sigma}}^D_{n+1}\|} |\mathrm{Tr}[\mathbf{K} \hat{\boldsymbol{\varepsilon}}^e_{n+1} \hat{\boldsymbol{\varepsilon}}^e_{n+1}]| \right] \mathrm{d}\Omega \\ & + \sum_{n=0}^{k} (t_{n+1} - t_n)^2 \int_\Omega \frac{1}{2} \mathrm{Tr}[\mathbf{K}^{-1} \hat{\boldsymbol{\sigma}}_{n+1} \hat{\boldsymbol{\sigma}}_{n+1}] + \frac{1}{2} \boldsymbol{\Lambda}^{-1} \hat{\boldsymbol{Y}}_{n+1} \circ \hat{\boldsymbol{Y}}_{n+1}\, \mathrm{d}\Omega \\ & + \int_\Omega \frac{1}{2} \mathrm{Tr}[\mathbf{K}^{-1} \hat{\boldsymbol{\sigma}}_{k+1} \hat{\boldsymbol{\sigma}}_{k+1}] + \frac{1}{2} \boldsymbol{\Lambda}^{-1} \hat{\boldsymbol{Y}}_{k+1} \circ \hat{\boldsymbol{Y}}_{k+1}\, \mathrm{d}\Omega \end{aligned} \tag{70}$$

### *6.3. Examples*

The space and time error indicators have ben calculated for the examples previously described. Tables 2 and 3 summarize the results. We note that:

- The time indicator is almost insensitive to the number of elements and approximates very well the time error.
- The space indicator barely depends on the number of time steps and approximates very well the space error.
- The space and time indicators decrease monotonically with respect to the number of elements and time steps, respectively.

In other words, space and time indicators do behave very well globally.

## 7. Conclusions

A new error, labeled the dissipation error, has been utilized in order to a posteriori estimate the errors committed in nonlinear time-dependent finite element computations for materials described by internal variables. This error, based on sound mechanical concepts, is directly linked to the gap occuring between the exact and approximate solutions.

Two error indicators have also been introduced to estimate the error due to either the space discretization or the time discretization solely. The time (space resp.) error indicator is the dissipation error associated with the reference problem discretized in space (time resp.). Satisfactory properties for the indicators have been demonstrated.

The error, as well as the indicators, will be used in a forthcoming paper to adapt both the time and space discretizations. A study of the influence on the error generated by the iterative technique will also be conducted.

## References


[1] J. Lemaitre and J.L. Chaboche, Mechanics of Solid Materials (Cambridge University Press, Cambridge, 1990).

[2] P. Ladevèze, Les bases de la méthode de l'erreur en relation de comportement pour le contrôle des calculus éléments finis: Les travaux des années 1975. Rapport interne 163, LMT, Ecole Normale Supérieure de Cachan, 1995.

[3] P. Ladevèze, J.P. Pelle and P. Rougeot, Error estimation and mesh optimization for classical finite element, Engrg. Comput. 8 (1991) 69–80.

[4] I. Babuska and W.C. Rheinboldt, A posteriori estimates for the finite element method, Int. J. Numer. Methods Engrg. 12 (1978) 1597–1615.

[5] I. Babuska and W.C. Rheinboldt, Adaptive approaches and reliability estimators in finite element analysis, Comput. Methods Applied Mech. Engrg. 17/18 (1979) 519–540.

[6] D.W. Kelly, J. Gago, O.C. Zienkiewicz and I. Babuska, A posteriori error analysis and adaptative processes in finite element method. Part 1: Error analysis, Int. J. Numer. Methods Engrg. 19 (1983) 1593–1619.

[7] J. Gago, D.W. Kelly, O.C. Zienkiewicz and I. Babuska, A posteriori error analysis and adaptative processes in finite element method. Part 2: Adaptative mesh refinement, Int. J. Numer. Methods Engrg. 19 (1983) 1921–1656.

[8] J.T. Oden, L. Demkowicz, W. Rachowicz and T.A. Westermann, Toward a universal *h-p* adaptative finite element strategy, Part 2: A posteriori error estimation, Comput. Methods Appl. Mech. Engrg. 77 (1989) 113–180.

[9] O.C. Zienkiewicz and J.Z. Zhu, A simple error estimator and adaptative procedure for practical engineering analysis, Int. J. Numer. Methods Engrg. 24 (1987) 337–357.

[10] O.C. Zienkiewicz and J.Z. Zhu, The superconvergent patch recovery and a posteriori error estimates, Part 1: The recovery technique, Int. J. Numer. Methods Engrg. 33 (1992) 1331–1364.

[11] O.C. Zienkiewicz and J.Z. Zhu, The superconvergent patch recovery and a posteriori error estimates, Part 2: Error estimates and adaptativity, Int. J. Numer. Methods Engrg. 33 (1992) 1365–1382.

[12] B. Fraeijs de Veubeke, Displacement and equilibrium models in the finite element method, in: O.C. Zienkiewicz, ed., Stress Analysis Chap. 9 (John Wiley, 1965).

[13] J.F. Debongnie, H.G. Zhong and P. Beckers, Dual analysis with general boundary conditions, Comput. Methods. Appl. Mech. Engrg. 122 (1995) 183–192.

[14] I. Babuska, T. Strouboulis, C.S. Upadhyay, S.K. Gangaraj and K. Copps, Validation of a posteriori error estimators by numerical approach, Int. J. Numer. Methods Engrg. 37 (1994) 1073–1123.

[15] I. Babuska, T. Strouboulis, S.K. Gangaraj and C.S. Upadhyay, Pollution-error in the *h*-version of the finite-element method and the local quality of a-posterior error estimators, Finite Elements Anal. Des. 17 (1994) 273–321.

[16] I. Babuska, T. Strouboulis, S.K. Gangaraj and C.S. Upadhyay, Validation of recipes for the recovery of stresses and derivatives by a computer-based approach, Math. Comput. Model. 20 (1994) 45–89.
[17] I. Babuska and W.C. Rheinboldt, Computational error estimates and adaptative processes for some nonlinear structural problems, Comput. Methods Appl. Mech. Engrg. 34 (1982) 895–937.
[18] C. Johnson and P. Hansbo, Adaptative finite element methods in computational mechanics, Comput. Methods Appl. Mech. Engrg. 101 (1992) 143–181.
[19] J.M. Bass and J.T. Oden, Adaptative finite element methods for a class of evolution problems in viscoplasticity, Int. J. Engrg. Sci. 25(6) (1987) 623–653.
[20] O.C. Zienkiewicz, Y.C. Liu and G.C. Huang, Error estimation and adaptativity in flow formulation for forming problems, Int. J. Numer. Methods Engrg. 25 (1988) 23–42.
[21] B. Tie and D. Aubry, Error estimates, *h* adaptative strategy and hierarchical concept for non linear finite element method, in: Ch. Hirsch et al., eds., Numerical Methods in Engineering '92 (Elsevier Science Publishers, 1992) 17–24.
[22] P. Ladevèze, Sur une famille d'algorithmes en mécanique des structures, Compte-Rendus de l'Académie des Sciences, Série II 300 (1985) 41–44.
[23] P. Ladevèze, G. Coffignal and J.P. Pelle, Accuracy of elastoplastic and dynamic analysis, in: I. Babuska, J. Gago, E. Oliveira and O.C. Zienkiewicz, eds., Accuracy Estimates and Adaptative Refinements in Finite Element Computations (J. Wiley, 1986) 181–203.
[24] L. Gallimard, P. Ladevèze and J.P. Pelle, Error estimation and adaptativity in elastoplasticity, Int. J. Numer. Methods Engrg. 39 (1996) 189–217.
[25] P. Ladevèze, La méthode à grand incrément de temps pour l'analyse de structures à comportement non linéaires décrit par variables internes, Compute-Rendus de l'Académie des Sciences, Série II 309(11) (1989) 1095–1099.
[26] P. Ladevèze, Mécanique non linéaire des structures. Nouvelle Approache et Méthodes de Calcul Non Incrémentales (Hermes, 1996).
[27] G. de Saxcé, Une généralisation de l'inégalité de Fenchel et ses applications aux lois constitutives, Compte-Rendus de l'Académie des Sciences, Série II 314 (1992) 125–129.
[28] A. Berga and G. Saxcé, Elastoplastic finite element analysis of soil problems with implicit standard material constitutive laws, Revue européenne de éléments Finis 3(3) (1994) 411–456.
[29] G. Duvaut and J.L. Lions, Les Inéquations en Mécanique et en Physique (Dunod, 1972).
[30] P. Ladevèze, Nouvelles procédures d'estimations d'erreur relative à la méthode des éléments finis, in: Proc. Journées Eléments Finis, Rennes, 1977.
[31] W. Prager and J.L. Synge, Approximation in elasticity based on the concept of functions space, Quart. Appl. Math. 5 (1947) 261–269.
[32] P. Ladevèze, La maîtrise des modèles en mécanique des structures, Revue européenne de éléments finis 1 (1992) 9–30.